

AD-752 218

A SEISMIC COMMUNICATIONS INVESTIGATION  
EMPLOYING A PIEZOELECTRIC TRANSDUCER

Craig C. Johnson

Southwest Research Institute

Prepared for:

Rome Air Development Center

September 1972

DISTRIBUTED BY:



National Technical Information Service  
U. S. DEPARTMENT OF COMMERCE  
5285 Port Royal Road, Springfield Va. 22151

AD752218

RADC-TR-72-241  
Final Technical Report  
September 1972



A SEISMIC COMMUNICATIONS INVESTIGATION  
EMPLOYING A PIEZOELECTRIC TRANSDUCER

Southwest Research Institute

Approved for public release;  
distribution unlimited.

1 D C C  
RECORDED  
PER  
100%  
100%  
100%

Rome Air Development Center  
Air Force Systems Command  
Griffiss Air Force Base, New York

NATIONAL TECHNICAL  
INFORMATION SERVICE

25A

## UNCLASSIFIED

Security Classification

## DOCUMENT CONTROL DATA - R &amp; D

(Security classification of title, body of abstract and indexing annotation must be entered when the overall report is classified.)

1. ORIGINATING ACTIVITY (Corporate author) Southwest Research Institute 8500 Culebra Road San Antonio, Texas 78284	2a. REPORT SECURITY CLASSIFICATION UNCLASSIFIED
	2b. GROUP

## 3. REPORT TITLE

A SEISMIC COMMUNICATIONS INVESTIGATION EMPLOYING A PIEZOELECTRIC TRANSDUCER

## 4. DESCRIPTIVE NOTES (Type of report and inclusive dates)

Final Report, November 1971 through July 1972

## 5. AUTHOR(S) (First name, middle initial, last name)

Craig C. Johnson

6. REPORT DATE September 1972	7a. TOTAL NO. OF PAGES 47 plus 7 Preliminaries	7b. NO. OF REFS 21
8a. CONTRACT OR GRANT NO F30602-72-C-0100	9a. ORIGINATOR'S REPORT NUMBER(S) 14-3261	
b. PROJECT NO. Job Order No.: R-1190000	9b. OTHER REPORT NO(S) (Any other numbers that may be assigned this report) RADC-TR-72-241	
c.		
d.		

## 10. DISTRIBUTION STATEMENT

Approved for public release.  
Distribution unlimited.

11. SUPPLEMENTARY NOTES	12. SPONSORING MILITARY ACTIVITY Rome Air Development Center Air Force Systems Command Griffiss Air Force Base, New York 13440
-------------------------	---

## 13. ABSTRACT

The purpose of this effort was to investigate the feasibility of employing a piezoelectric transducer for seismic communications applications in mine environments. The transducer, a GFE device, incorporated a high Q, spring-mass resonator to load the air side of the piezoelectric crystal. The resonant frequency was seismic load dependent and fell in the range of 300 to 340 Hz. The effort included a mathematical analysis of the transducer, with corroborative laboratory tests, together with actual communications experiments performed first in an open-formation limestone quarry and finally in an operating iron mine. This work showed that the transducer could be coupled efficiently to hard, competent rock media with power conversion efficiencies of 70 to 80 percent (electrical to mechanical) in typical installations. In the iron mine, when radiating peak power was about 30 W (acoustical) in a gated pulse mode, signals were received at a distance of 760 ft. through a massive rhyolite porphyry formation. This represents a 15% radiation efficiency with an input of 200 watts. Despite the high ambient noise level due to operating machinery, a signal-to-noise ratio of about 20 dB was achieved using a very narrow band filter to process the received signal, and a data rate of about two pulses/sec was demonstrated.

Details of illustrations in  
this document may be better  
studied on microfiche.

DD FORM 1473

I-A

UNCLASSIFIED

Security Classification

**UNCLASSIFIED**

Security Classification

14

KEY WORDS	LINK A		LINK B		LINK C	
	ROLE	WT	ROLE	WT	ROLE	WT
Seismic Communications						
Seismic Propagation						
Piezoelectric Transducer						
Sensors						
Modulation						

I-B

UNCLASSIFIED

Security Classification

A SEISMIC COMMUNICATIONS INVESTIGATION  
EMPLOYING A PIEZOELECTRIC TRANSDUCER

Craig C. Johnson

Southwest Research Institute

Approved for public release;  
distribution unlimited.

Do not return this copy. Retain or destroy.

I-C

## FOREWORD

This work was performed by Southwest Research Institute, P.O. Drawer 28510, San Antonio, Texas, 78228, and was supported jointly by the U.S. Department of the Interior, Washington, D.C., 20240, and the Air Force Systems Command, Rome Air Development Center, Griffiss Air Force Base, N.Y., 13440. Administration of the contract was handled by RADC under Contract No. F30602-72-C-0100, and Mr. Alfred D. Paoni, RADC/COAL, was the technical program monitor. The program was also identified as RADC Project R-1190000 and by the contractor's in-house project designation 14-3261.

Technical effort was initiated by the contractor in November 1971 and completed in July 1972. The final report was submitted in August 1972.

The communications experiments in the field could not have been performed without the permission, interest, cooperation, and assistance of the U.S. Gypsum Co., New Braunfels, Texas, Plant Mr. D.J. George, works manager; and the Meramec Mining Co., Sullivan, Mo., 63080, Mr. R.G. Peets, resident manager.

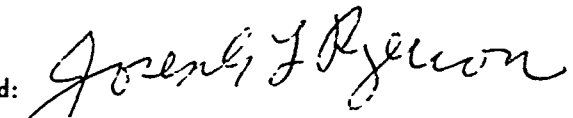
Of the several people who contributed to this effort at Southwest Research Institute, it will suffice to mention Dr. T.E. Owen, who provided significant technical guidance and advice; Mr. E.A. Brown, who served as geological consultant; and Mr. G.W. Kirk, who was largely responsible for the successful acquisition of field test data.

This technical report has been reviewed and is approved.



Approved: ALFRED D. PAONI  
Project Engineer

Approved:



JOSEPH L. RYERSON, Technical Director  
Communications and Navigation Division

FOR THE COMMANDER:

  
FRED I. DIAMOND  
Acting Chief, Plans Office

## TABLE OF CONTENTS

	<u>Page</u>
I. INTRODUCTION . . . . .	1
II. PERFORMANCE ANALYSIS OF TRANSDUCER . . . . .	3
1. Initial Analysis and Equivalent Circuit . . . . .	3
2. Performance Equations . . . . .	6
3. Impedance Matching . . . . .	9
4. Simplified Equivalent Circuit and Performance Equations . . . . .	9
5. The Transducer as a Receiver . . . . .	11
6. Laboratory Tests . . . . .	12
III. EXPERIMENTAL EQUIPMENT . . . . .	20
1. General Arrangement . . . . .	20
2. Drive Transformer . . . . .	20
3. Control Circuit . . . . .	24
IV. LIMESTONE QUARRY EXPERIMENTS . . . . .	25
1. Test Site Description . . . . .	25
2. Test Results . . . . .	28
V. IRON MINE EXPERIMENTS . . . . .	31
1. General Description and Arrangements . . . . .	31
2. Test Results . . . . .	32
3. Laboratory Signal Processing . . . . .	36
4. Signal Attenuation with Range . . . . .	38
VI. CONCLUSIONS AND RECOMMENDATIONS . . . . .	39
APPENDIX—DERIVATION OF PIEZOELECTRIC CRYSTAL EQUIVALENT CIRCUIT . . . . .	41

## LIST OF ILLUSTRATIONS

<u>Figure</u>		<u>Page</u>
1	RADC Transducer, Idealized Cross Section . . . . .	3
2	Transducer Mechanical Schematic . . . . .	5
3	Equivalent Circuit Representation, RADC Transducer Driving Seismic Load . . . . .	7
4	Simplified Equivalent Circuit Representation RADC Transducer Driving Seismic Load . . . . .	10
5	Frequency Response RADC Transducer Infinitely Stiff Load (Back-to-Back) . . . . .	13
6	RADC Transducer, Radiated Power . . . . .	15
7	RADC Transducer, Efficiency and Bandwidth . . . . .	15
8	Frequency Response RADC Transducer Concrete Pier Load . . . . .	18
9	Local Transmitter Test Arrangement . . . . .	21
10	Transmitter Unit, Propagation Tests . . . . .	21
11	Receiver Unit, Propagation Tests . . . . .	22
12	Local Transmitter Test Equipment . . . . .	22
13	Transmitter Unit Test Equipment . . . . .	23
14	Receiver Unit Test Equipment . . . . .	23
15	Control Box—Simplified Schematic . . . . .	24
16	Limestone Quarry Test Site . . . . .	25
17	Limestone Quarry—Receiver Transducer Installation . . . . .	26
18	Typical Transducer Mounting Pad . . . . .	26
19	Limestone Quarry—Transmitter Site No. 1 . . . . .	27
20	Limestone Quarry—Typical Transmission (450-Ft Path) . . . . .	29
21	Limestone Quarry—Impulse Response (450-Ft Path) . . . . .	30
22	Pea Ridge Mine—Idealized Geological Section . . . . .	31
23	Iron Mine—Transmitter Installation, 2475 Level . . . . .	33
24	Iron Mine—Typical Received Signals, 2275 Level . . . . .	34
25	Iron Mine—Typical Received Signals, 2275 Level . . . . .	34

## LIST OF ILLUSTRATIONS (Cont'd)

<u>Figure</u>		<u>Page</u>
26	Iron Mine—Receiver Installation, 1825 Level . . . . .	35
27	Iron Mine—Typical Received Signals, 1825 Level . . . . .	36
28	Iron Mine—Narrow Band Filtering, 2275 Level . . . . .	37
29	Iron Mine—Narrow Band Filtering, 1825 Level . . . . .	37
30	Iron Mine—Narrow Band Filtering, 1825 Level . . . . .	38

Evaluation - Seismic Comm. F30602-72-C-0100

This effort was pursued in support of a short range communication system in rock strata. The task is covered in RADC TP0-10, Radio Communications. SAMSO TN-21-67-08 entitled "Short Range Telluric Transmission System," has a need for developing a two way, short range communication system between missile silos and hardened cables. The primary requirement in Seismic communications is to develop a repeatable and efficient source (transmitter). The transducer evaluated under this effort substantiates the design technique as being qualified and meaningfully efficient for hard rock application. The anticipated promise of the piezoelectric transducer of reasonable size and weight, together with a 50% radiation efficiency, has been a realizable goal with the knowledge gained from the aforementioned effort.



ALFRED D. PAONI  
RADC Project Engineer

## SECTION I

### INTRODUCTION

The purpose of the work reported herein was to investigate the feasibility of employing piezoelectric transducers for seismic communications and exploratory mapping purposes in mine environments. The emphasis upon mine environments implies that conditions of interest are those involving seismic transmission paths or at least one terminus of such a path deep within the interior of massive rock (or coal) formations. This distinction is of significance since seismic propagation by surface waves is thus largely precluded.

The efficacy of a convenient exploratory mapping system in mine operations, tunnel driving, etc., is rather obvious; correspondingly, a means for communications through perhaps many hundreds of feet of rock could be of tremendous benefit in mine emergencies wherein entrapped miners, otherwise cut off from normal communications, could communicate with rescue teams elsewhere in the mine and on the surface. Moreover, such a means might be of general value in mine and tunnel driving operations, permitting the transmission of operational messages into the far reaches, unencumbered by the need for pulling in, hanging, and protecting vulnerable wire lines. Another important application would be that of providing redundant, damage-resistant channels of communication in defense applications, such as underground command headquarters, etc. Other applications beyond those mentioned are also conceivable.

The investigation reported here is not to be regarded as a comprehensive treatment of the problem of adapting piezoelectric transducers to the purposes mentioned above. Rather, this was a somewhat specific investigation in which a government-furnished transducer was employed. The results, then, reflect the performance capabilities of this transducer, which will be described later in detail, although, through analysis and evaluation, it appears reasonable to extrapolate these findings to a general class of piezoelectric transducer. The government-furnished transducer, which was designed and fabricated by others, is a highly resonant or high Q-type device, operating at a frequency of 300 to 340 Hz but not lending itself to the generation of sharp impulse signals. Consequently, its usefulness in exploratory mapping work is very dubious, since, for such work, a very sharp impulse or high frequency, gated pulse propagated into the medium is normally required. Only in this way can the return echoes from various layers, inclusions, etc. be resolved timewise from the transmit pulse and presented for interpretation. Continuous wave exploratory mapping techniques are theoretically possible, of course, but, because of the complexity of multimode propagation phenomena, such methods are not considered generally practicable. This does not imply, however, that piezoelectric transducers could not be employed for mapping applications, for, in fact, a suitably designed, broadband unit capable of propagating sharp impulse signals would probably be the preferred selection for such work. Such units have indeed been developed. At any rate, the transducer employed herein did not appear suitable for the mapping application; therefore, the effort was centered upon the communication application.

The investigation included theoretical analysis of the transducer, backed by corroborative laboratory tests, for the purpose of arriving at a comprehensive understanding of the performance of the unit functioning as a source into rock media. Operating characteristics such as efficiency, bandwidth, radiated power, impedance matching to the rock interface, etc. were of primary interest. This work was followed by communications experiments in both an open-formation limestone quarry and an operating iron mine. In this work, tests were performed to determine operating range, signal-to-noise

ratios, effect of fractured formations, potential data rates, propagation velocity and attenuations, etc. These various characteristics, taken together with practical considerations related to equipment design, etc., constitute the sort of information required to evaluate the feasibility of this communications method.

To provide some guidance to this effort, a brief survey of the open literature was performed. Owen<sup>(1)\*</sup> presents a rather comprehensive theoretical treatment of seismic propagation in layered media, with the added considerations of controlled seismic sources, received-signal processing, communications systems concepts, etc., together with a rather complete survey of the open literature up to 1964. In the vast literature covering all aspects of seismic propagation and the design and application of piezoelectric transducers, there are relatively few references directly pertaining to this investigation. As cited by Owen, the first efforts of significance employing a controlled seismic source were reported in a series of papers by Evison<sup>(2-7)</sup> in the period 1951 to 1956. He used a broadband electrodynamic source which exhibited very poor coupling efficiency but successfully transmitted gated pulse signals in the 100- to 600-Hz range, over distances of several hundred feet, in chalk mines and tunnels, and on stratified surface layers. Pursey<sup>(8,11)</sup> and Miller and Pursey<sup>(9,10)</sup> provide theoretical formulations for the field and radiation impedance, partition of energy, and power radiated by a source on the surface of a semi-infinite isotropic solid; thus, they laid the groundwork for an understanding of the coupling and propagation problems. Later, Ikrath, et al<sup>(12-15)</sup> reported a series of investigations in the 1963 to 1966 period employing a resonant-type electrodynamic source (most work was done at 80 Hz), with propagation along surface layers of the earth, ice-covered lakes, etc. The coupling efficiency of this transducer was quite good, and satisfactory signals were received at distances of hundreds of meters. Further work with transmitter arrays was also reported. Zeitz and Pakiser<sup>(16)</sup> cover briefly and incompletely the application of a sonar-type transmitter for exploratory mapping work (grease and water coupled to the earth and, operating at frequencies of 6, 11.5, and 16 kHz).

Regarding piezoelectric transducer design, McMaster, et al<sup>(17)</sup> for example, did extensive work in high-power applications, covering such features as impedance matching, crystal preloading, cooling, etc. for units operating up to peak power outputs of 30 kW at frequencies of 10 kHz or higher. It should be noted, however, that none of these previous efforts has been concerned with the design and employment of piezoelectric transducers for the specific application of communication through rock media. However, it is also evident that this application is one of adaptation only, since the various elements of seismic propagation and piezoelectric transducer design have reached a high level of technical maturity over the past years. Accordingly, the chief concern of the effort reported here was to shed light, both qualitatively and quantitatively, on the feasibility of just such an adaptation.

---

\*Superscript numbers in parentheses refer to References at the end of this report.

## SECTION II

### PERFORMANCE ANALYSIS OF TRANSDUCER

#### 1. INITIAL ANALYSIS AND EQUIVALENT CIRCUIT

So that a comprehensive understanding of the behavior of the piezoelectric transducer could be acquired, a mathematical analysis of this unit was performed. The initial analysis effort was augmented by results of corroborative laboratory tests on the transducer so that a quantitative mathematical model was constructed. From this model, it was then possible to calculate performance characteristics such as radiated power, bandwidth, and efficiency as a function of arbitrary seismic load. These results in turn provided the basis for the rational application of the transducer in communications experiments in actual field environments. A discussion of the development of the mathematical model follows after a brief description of the physical characteristics of the transducer.

The piezoelectric transducer, two of which were furnished by the government for this work, was manufactured by the Redford Corp., Latham, N.Y., under the designation of Model 2427, and it has been further designated as RADC Model T-100. In this report, the unit will be referred to simply as the RADC transducer. Figure 1 depicts an idealized cross section of the transducer. The piezoelectric crystal stack consists of six Vernitron 56131 (PZT-4 ceramic) crystals bonded together

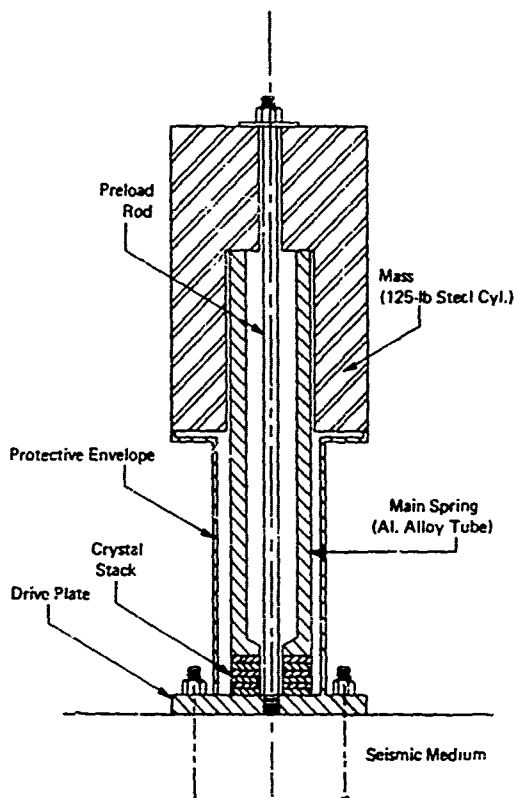


FIGURE 1. RADC TRANSDUCER, IDEALIZED CROSS SECTION

and connected in electrical parallel. They are polarized and driven in the thickness mode, which is parallel to the long axis of the transducer. One end of the crystal stack is held firmly to the rock interface via the drive plate, using anchor bolts or other appropriate means, while the other end is loaded by the spring-mass system. When the crystal is driven at the resonant frequency of the spring-mass system, the mechanical impedance at the spring-mass crystal face becomes very high (provided the Q of the resonance is high), thus permitting more of the available energy to propagate into the rock. The spring-mass system can also be viewed, heuristically at least, as a quarter wavelength transmission line. It is this resonant drive feature that permits the unit to couple efficiently to the seismic medium. The resonant frequency is in the range of about 300 to 340 Hz, a value which is sensitive to the installation and which cannot be altered. This resonant frequency range was probably selected by the designer as a compromise between radiated power capability and anticipated signal attenuation rates in seismic media; results of the effort here appear to support that selection generally. It is mandatory that a piezoelectric crystal never be allowed to operate in tension; thus, a compressive preload must be applied that always exceeds the maximum operating peak tension load. This preload is provided by the rod shown in Figure 1, and, for this design, this same loaded rod is used to couple the crystal stack, spring, and mass. Since the peak dynamic load of the unit is on the order of 5000 lb, the rod preload must exceed this value by a comfortable margin. Similarly, the transducer must be affixed to the seismic medium with a load exceeding 5000 lb to assure continuous contact. According to the manufacturer's manual, terminal voltage on the crystal is limited to 1500 V rms. In envelope dimensions, the unit is about 24 in. long and 7 in. in diameter, weighing about 150 lb.

From the physical configuration of the transducer described above, a functional, mechanical schematic of the unit is suggested, as shown in Figure 2 along with a definition of symbols. It is noted that the crystal stack is depicted simply as a force generator in which the force,  $F_c$ , is applied to the external mechanical elements. (The spring rate of the protective envelope is negligible compared to other springs in the system.) By examination, it is possible to write the following expressions:

$$\begin{aligned} F_c &= m\ddot{x} + (\dot{x} + \dot{y}_2)b_r + (x + y_2)k_r \\ F_c &= (\dot{y}_1 - \dot{x})b + (y_1 - x)k \\ F_c &= \dot{y}_2 b_s + y_2 k_s + (\dot{x} + \dot{y}_2)b_r + (x + y_2)k_r \end{aligned} \quad (1)$$

where overdotting of a quantity indicates a time derivative. It is convenient to work with the concept of mechanical impedance defined as the vector ratio of force to velocity. Accordingly, assuming sinusoidal time variation with radian frequency,  $\omega$ , and defining

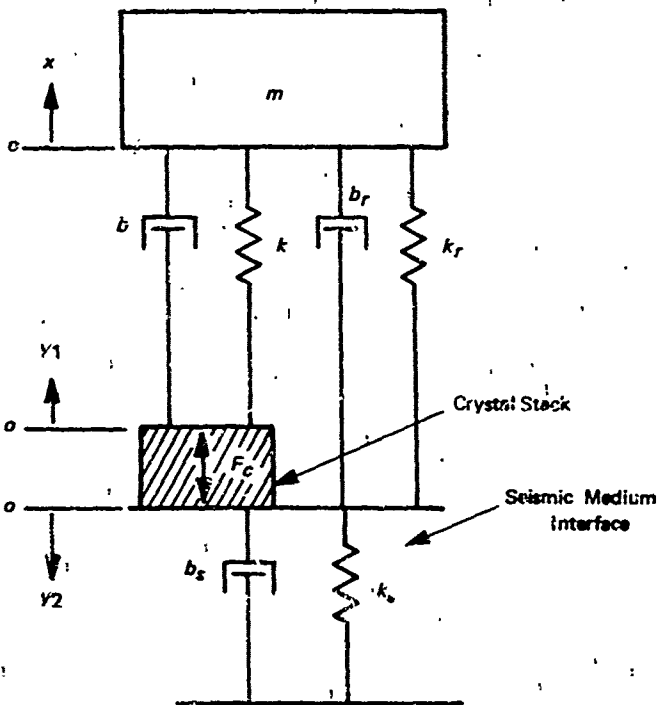
$$v_1 = \dot{y}_1 = j\omega y$$

$$v_2 = \dot{y}_2 = j\omega y_2$$

$$v_m = \dot{x} = j\omega x$$

Eqs. (1) can be rewritten:

$$\begin{aligned}
 F_c &= j\omega m v_m + \left( b_r + \frac{k_r}{j\omega} \right) (v_m + v_2) \\
 F_c &= \left( b + \frac{k}{j\omega} \right) (v_1 - v_m) \\
 F_c &= \left( b_s + \frac{k_s}{j\omega} \right) v_2 + \left( b_r + \frac{k_r}{j\omega} \right) (v_m + v_2)
 \end{aligned} \tag{2}$$



- $m$  ~ mass
- $k$  ~ spring rate constant, mainspring
- $b$  ~ viscous damping constant, mainspring
- $k_r$  ~ spring rate constant, preload rod
- $b_r$  ~ viscous damping constant, preload rod
- $k_s$  ~ equivalent spring rate constant, seismic medium
- $b_s$  ~ equivalent viscous damping, seismic medium
- $x$  ~ displacement of mass
- $y_1$  ~ displacement of upper crystal face
- $y_2$  ~ displacement of lower crystal face
- $F_c$  ~ crystal output force

FIGURE 2. TRANSDUCER MECHANICAL SCHEMATIC

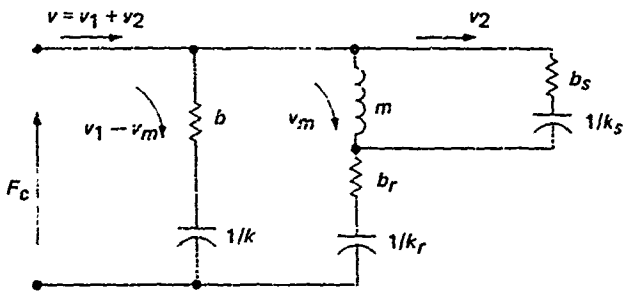
If we further postulate an electrical to mechanical analogy, such that

voltage $\rightarrow$ force
current $\rightarrow$ velocity
charge $\rightarrow$ displacement

which also implies, derivatively,

inductance  $\rightarrow$  mass  
 capacitance  $\rightarrow$  inverse spring rate  
 resistance  $\rightarrow$  viscous damping

Then we can transform the mechanical representation into a sort of an equivalent "electrical" circuit as follows:



In the Appendix, the equivalent circuit development for the piezoelectric crystal stack is presented, and it is quite easy to incorporate that result directly into the above development. The resulting overall equivalent circuit for the transducer operating into a seismic medium is shown in Figure 3. It should be carefully observed that all quantities to the left of the ideal electrical-to-mechanical transformer are electrical, while all quantities to the right are mechanical. No loss in meaning is to be implied by the substitution of  $R$ ,  $L$ , and  $C$  designators to the mechanical elements on the right side in place of  $b$ ,  $m$ , and  $1/k$  designators, respectively. Note also that a parallel representation of the seismic load is employed. A simple, lumped constant representation for the seismic load is valid in general only for a very narrow frequency range, in this case in the vicinity of resonance. The parallel resistance element,  $R_p$ , is to be regarded as the radiation resistance of the seismic medium, but this also accounts for acoustic energy radiated from the resonant mass element and frictional losses that might occur in the source-medium interface region as a result of nonlinear coupling phenomenon. For coupling to "hard" rock media, this latter is considered negligible so long as stress levels in the rock do not become excessive. Note also that the reactive part of the seismic load need not necessarily be capacitive, for it can as well be inductive.

## 2. PERFORMANCE EQUATIONS

From the equivalent circuit presented in Figure 3, it is possible to develop all the relationships required to characterize the performance of the transducer operating into a seismic load. The quantities of interest are the force generated against the seismic medium,  $F_m$ , power radiated into the medium, power conversion efficiency, and information bandwidth. This effort is not concerned with

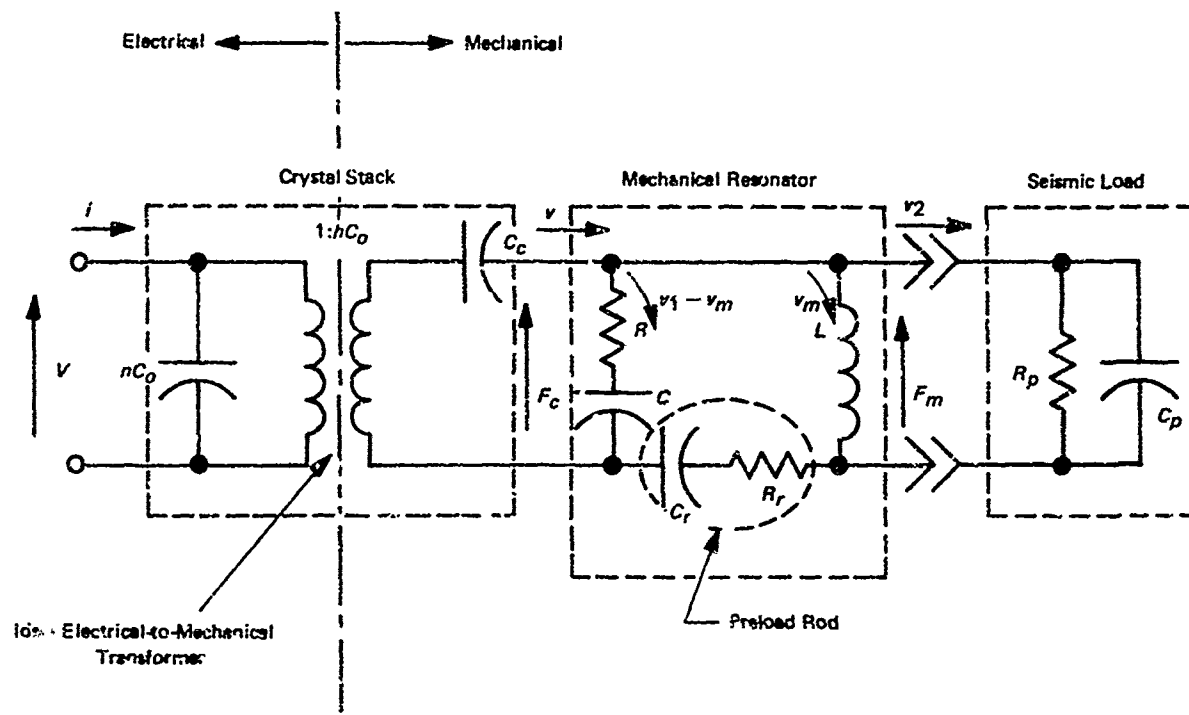


FIGURE 3. EQUIVALENT CIRCUIT REPRESENTATION, RADC TRANSDUCER  
DRIVING SEISMIC LOAD

the design and performance of the drive amplifier and associated elements since this is considered straightforward. Such equipment assembled to perform the various tests will be described later.

The transfer function relating the output force,  $F_m$ , to the input drive voltage,  $V$ , is given in the following expression where  $s$  is the Laplacian operator and the variables are understood to be  $s$ -domain variables:

$$\frac{F_m}{V} = \frac{hC_o \left( \frac{C_r}{C_c + C + C_r} \right) LC_c s^2 (RCs + 1)}{As^4 + Bs^3 + Cs^2 + Ds + 1} \quad (3)$$

where:

$$A = \frac{LC_c CC_r C_p RR_r}{C_c + C + C_r}$$

$$B = L \left[ \frac{C_c CC_r R \left( 1 + \frac{R_r}{R_p} \right) + C_c C_p (CR + C_r R_r) + CC_r C_p (R + R_r)}{C_c + C + C_r} \right]$$

$$C = L \left[ \frac{C_c CR}{R_p (C_c + C + C_r)} + \frac{C_c C_r \left( 1 + \frac{R_r}{R_p} \right) + CC_r \left( 1 + \frac{R}{R_p} + \frac{R_r}{R_p} \right)}{C_c + C + C_r} \right] + C_p + \frac{C_c CC_r RR_r}{C_c + C + C_r}$$

$$D = \frac{L}{R_p} + \frac{C_c CR + C_r(C_c R_r + CR + CR_r)}{C_c + C + C_r}$$

This is a rather formidable expression, but, fortunately, because of the range of numerical values employed and in the vicinity of resonance, the transfer function is given to a close approximation by

$$\frac{F_m}{V} \approx \frac{\frac{hC_o}{C_c + C + C_r} \left( \frac{C_r}{C_c + C + C_r} \right) L C_c s^2}{L \left[ \frac{C_r(C_c + C)}{C_c + C + C_r} + C_p \right] s^2 + \left[ \frac{L}{R_p} + \frac{C C_r(R + R_r)}{C_c + C + C_r} \right] s + 1} \quad (4)$$

Moreover, since the transducer must operate at resonance to couple efficiently to the seismic medium, the magnitude of  $F_m$  can be determined from Eq. (4) by substituting everywhere  $j\omega$  for  $s$  and setting  $\omega$  at the value required for resonance. This becomes, for a high Q resonance,

$$F_{m_{res}} \approx \frac{\frac{hC_o V}{C_c + C + C_r} \left( \frac{C_r}{C_c + C + C_r} \right) L C_c j\omega}{\frac{L}{R_p} + \frac{C C_r(R + R_r)}{C_c + C + C_r}} \quad (5)$$

where  $\omega$ , the resonant radian frequency, is given by

$$\omega = \frac{1}{\sqrt{L \left[ \frac{C_r(C_c + C)}{C_c + C + C_r} + C_p \right]}} \quad (6)$$

Note that  $F_m$  and  $V$  are no longer  $s$ -domain variables in Eq. (5). The power radiated into the seismic load is given as

$$P_{rad.} = \frac{|F_m|^2}{R_p} \quad (7)$$

where  $|F_m|$  is given in rms units.

To obtain power conversion efficiency, it is necessary to determine the losses in the transducer that result from the two lossy elements  $R$  and  $R_r$ . These two losses are given by

$$P_{loss} = \frac{|F_c|^2 (RC\omega)^2}{R} + |F_m|^2 \left( \frac{R_r}{L\omega} \right)^2 \frac{1}{R_r}$$

The relationship between  $F_c$  and  $F_m$  is rather complex, but, for typical numerical values employed here, sufficient accuracy is achieved by setting  $|F_c| = (0.84)|F_m|$ . The above equation can then be written

$$P_{loss} = |F_m|^2 \left[ \frac{(0.706)(RC\omega)^2}{R} + \frac{1}{R_r} \left( \frac{R_r}{L\omega} \right)^2 \right] \quad (8)$$

As before,  $|F_m|$  is given in rms units. The efficiency of power conversion,  $\epsilon_p$ , is defined as follows:

$$\epsilon_p = \frac{P_{\text{rad}}}{P_{\text{rad}} + P_{\text{loss}}} \quad (9)$$

The information bandwidth is defined as the bandwidth at the half power points (-3-dB points). This is given as

$$BW = \left[ \frac{L}{R_p} + \frac{CC_r(R + R_r)}{C_c + C + C_r} \right] \frac{\omega^2}{2\pi}, \text{ Hz} \quad (10)$$

As verified by laboratory tests, numerical values for all quantities are presented in a later section of this report, and performance calculations are presented in the form of curves for arbitrary seismic load.

### 3. IMPEDANCE MATCHING

For the applications envisioned here, it is desirable to minimize power supply requirements and the weight and bulk volume of the equipment. Thus it becomes important to examine the impedance matching problem since it is well known that maximum power transfer occurs when the source and load impedances are matched. If we take the derivative of  $P_{\text{rad}}$  as given in Eq. (7) with respect to  $R_p$  and set the result to zero, we obtain the expression for the value of  $R_p$  required to maximize  $P_{\text{rad}}$ . This is

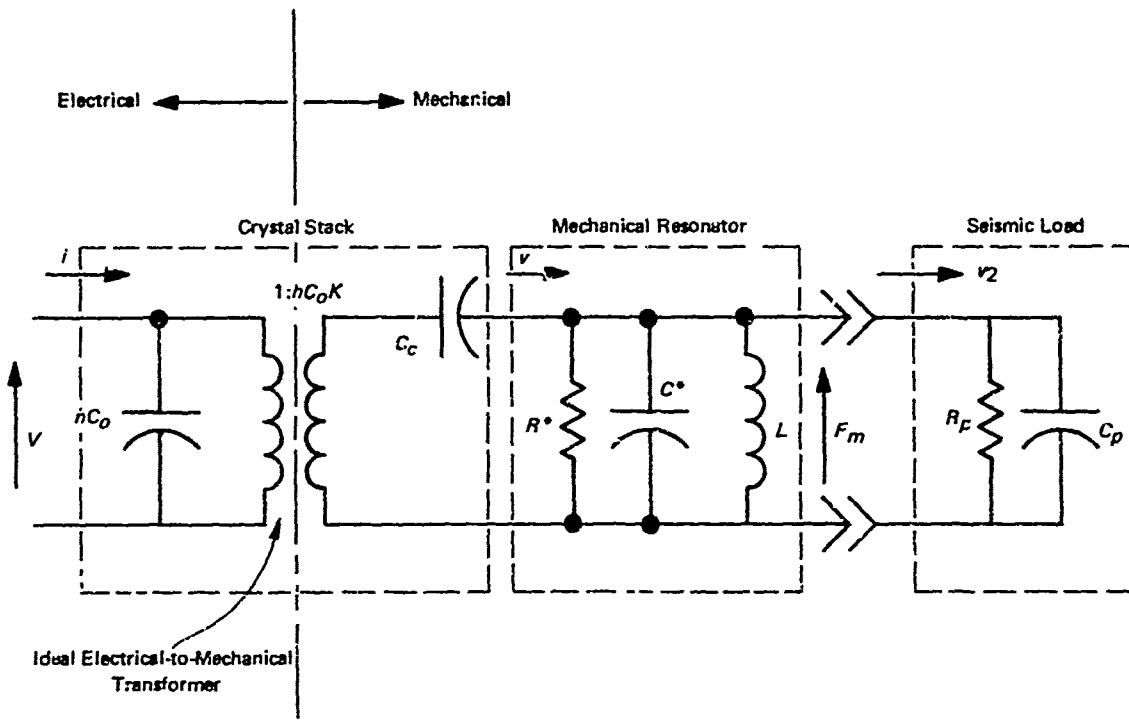
$$R_{p_{\text{opt}}} = \frac{L(C_c + C + C_r)}{CC_r(R + R_r)} \quad (11)$$

Although not presented here, it can be shown that this value of  $R_p$  also results in the correct conjugate complex impedance match between the seismic load and the source transducer, the only other requirement being that the resonant radian frequency,  $\omega$ , be that as given by Eq. (6). From this fact it is clear that the resonant frequency is sensitive to the reactive part of the seismic load. As shown by Miller and Pursey<sup>(9)</sup> and as verified by work under this contract, the reactive part of the radiation impedance is typically capacitive where the dimensions of the source are small compared to the shear wavelength in the medium. If, under other circumstances, the reactive part happened to be inductive, the equations could readily be rewritten. Then the attachment of the transducer to the seismic load would result in an increase in the resonant frequency as compared to the isolated transducer resonance, rather than in the decrease experienced with capacitive-type loads.

Miller and Pursey<sup>(9)</sup> also show that the magnitude of the radiation impedance becomes greater as the diameter of the interface drive disk is increased. This implies that use might be made of area transforming "horns" between the transducer and the seismic medium as a means of obtaining better impedance matching. From a practical standpoint in the case at hand, this could be accomplished only in the direction of increasing the area at the seismic medium end of the horn, and this would rapidly lead to very heavy and bulky horns with considerably aggravated mounting problems.

### 4. SIMPLIFIED EQUIVALENT CIRCUIT AND PERFORMANCE EQUATIONS

For the range of numerical values encountered here and in the vicinity of resonance, the equivalent circuit given in Figure 3 can be replaced with the simplified equivalent circuit presented in Figure 4.



Note:  $K = \frac{C_r}{C_c + C + C_r}$  from Equivalent Circuit, Figure 3

FIGURE 4. SIMPLIFIED EQUIVALENT CIRCUIT REPRESENTATION RADC TRANSDUCER DRIVING SEISMIC LOAD

Using this circuit, the corresponding performance equations are as follows:

$$F_{m_{res}} \approx KhC_o VC_c \left( \frac{R^* R_p}{R^* + R_p} \right) j\omega \quad (12)$$

$$\omega = \frac{1}{\sqrt{L(C_c + C^* + C_p)}} \quad (13)$$

$$P_{rad} = \frac{F_m^2}{R_p} \quad (14)$$

$$P_{loss} = \frac{|F_m|^2}{R^*} \quad (15)$$

$$\epsilon_p = \frac{P_{rad}}{P_{rad} + P_{loss}} \quad (16)$$

$$BW = \frac{L(R^* + R_p) \omega^2}{R^* R_p} \frac{1}{2\pi}, \text{ Hz} \quad (17)$$

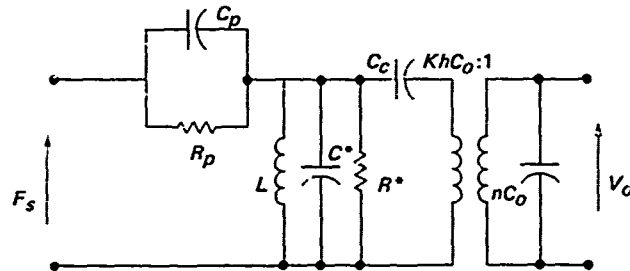
$$R_{p \text{ opt}} = R^* \quad (18)$$

From a conceptual point of view, this simplified model is more satisfying, and performance calculations are less time consuming. The overall results are identical with those obtained with the more complete expressions. It should be noted that the factor  $K$  is derived from the comprehensive circuit and is given as

$$K = \frac{C_r}{C_c + C + C_r} \quad (19)$$

## 5. THE TRANSDUCER AS A RECEIVER

In all that has gone before, the RADC transducer has been viewed only as a source or transmitter for the purpose of radiating energy into the seismic medium. To be sure, this is the matter of most direct concern here, since a variety of small, low-power, highly sensitive instruments is available for the detection of seismic vibrations. Nevertheless, the RADC transducer can be employed as a receiving device of great sensitivity, and it is certainly conceivable and manifestly convenient that a single such unit at a given site be used for both transmitting and receiving. The equivalent circuit for the unit operating as a receiver is as shown here:



The seismic disturbance is viewed here as a force input,  $F_s$ , while the output is a voltage,  $V_o$ , a high impedance detector implied. All other circuit elements are as shown in Figure 4. The  $s$ -domain transfer function in the vicinity of resonance is, approximately,

$$\frac{V_o}{F_s} \approx \frac{\left( \frac{LKhC'}{R_p n} \right) s (R_p C_p s + 1)}{L(C_p + C^* + C') s^2 + L \left( \frac{1}{R_p} + \frac{1}{R^*} \right) s + 1} \quad (20)$$

where

$$C' = \frac{n C_c}{n + K^2 h^2 C_o C_c}$$

Or, at resonance, substituting  $j\omega$  everywhere for  $s$ , there results

$$\frac{V_o}{F_s} \approx \sqrt{\frac{KhC'}{n}} \left( \frac{R^*}{R_p + R^*} \right) (1 + j\omega R_p C_p) \quad (21)$$

In this form, this is quite similar to Eq. (12), and it is noted that high sensitivity is predicated upon high Q resonance. In this case, the resonant frequency contains an effect due to the capacitor across the crystal terminals,  $nC_o$ . However, this can be tuned out with an inductor, and the sensitivity can be increased several decibels depending on the Q of the inductor. It should be clear that the resonant frequency of the receiver unit be within a few hertz of the resonant frequency of the transmitter unit in order to establish effective communications.

## 6. LABORATORY TESTS

### a. Piezoelectric Crystal

Laboratory tests on the transducer were devised for the purpose of verifying the form of the mathematical model (or the equivalent circuit) and quantifying numerical values of the various elements. The first set of tests was designed to determine the values of  $C_o$ ,  $h$ , and  $C_c$  for the crystal stack. These quantities are defined in the Appendix. The crystal stack was driven over the frequency range of 300 to 400 Hz with an air load on one face. This, in effect, short circuits the mechanical resonator and seismic load in Figure 3. This forces  $F_c = 0$  in Eq. (28), Appendix, and, together with Eq. (27) and considerable manipulation, it is found that

$$C_o = \frac{1}{\left(\frac{v}{i}\right)^2 k + \frac{n}{C'}} \quad (22)$$

$$h = \frac{i}{C_o v} \left(1 - \frac{nC_o}{C'}\right)$$

where

$$C' = \frac{i}{j\omega v}$$

Thus, the test requires the measurement of  $V$ ,  $\omega$ ,  $i$ , and  $v$  (the velocity on the air-loaded face). Also needed is the value of  $n = \epsilon$  and the calculated value of  $k = 4.58 \times 10^{10}$  N-m for the PZT-4 crystal stack spring rate. From these data, values for  $C_o$  and  $h$  were then calculated. On the following page, the results for each of the transducers are tabulated and compared to overall theoretical values calculated from manufacturers' data. It is felt that these results, which required very careful measurements, demonstrate the adequacy of the assumed model and provide good numerical values for purposes of calculations.

### b. Mechanical Resonator

The next test was designed to verify and quantify the mechanical resonator portion of the model. At first glance, this appeared elementary; however, the spring rate of the main resonator

Quantity	Trans. No. 30	Trans. No. 31	Theoretical
$C_o, \mu F$	0.00227	0.00213	0.00204
$h, V/m \times 10^9$	2.70	2.94	3.15
$hC_o, N/V$	6.12	6.26	6.42
$nC_o, \mu F$	0.0136	0.0128	0.0122
$C_c, m/N \times 10^{-10}$	2.05	2.27	2.35
$\zeta', \mu F$	0.0212	0.0215	0.0219

spring was found to be of the order of  $10^6$  lb/in. such that there was simply nothing "stiff" enough against which this spring-mass system might be referenced for measurement purposes without also affecting the resonance and Q of the system. The solution was to mount the two transducers back-to-back and drive them in parallel. In this arrangement, assuming that the two units are well matched in dynamic properties, the interface between the two units appears as a nearly infinitely "stiff" reference, and the resulting measurements of resonant frequency and Q are representative of the isolated mechanical resonator. Accordingly, this test was performed with typical results presented in Figure 5. This is a frequency response curve presenting the ratio of output force to input drive

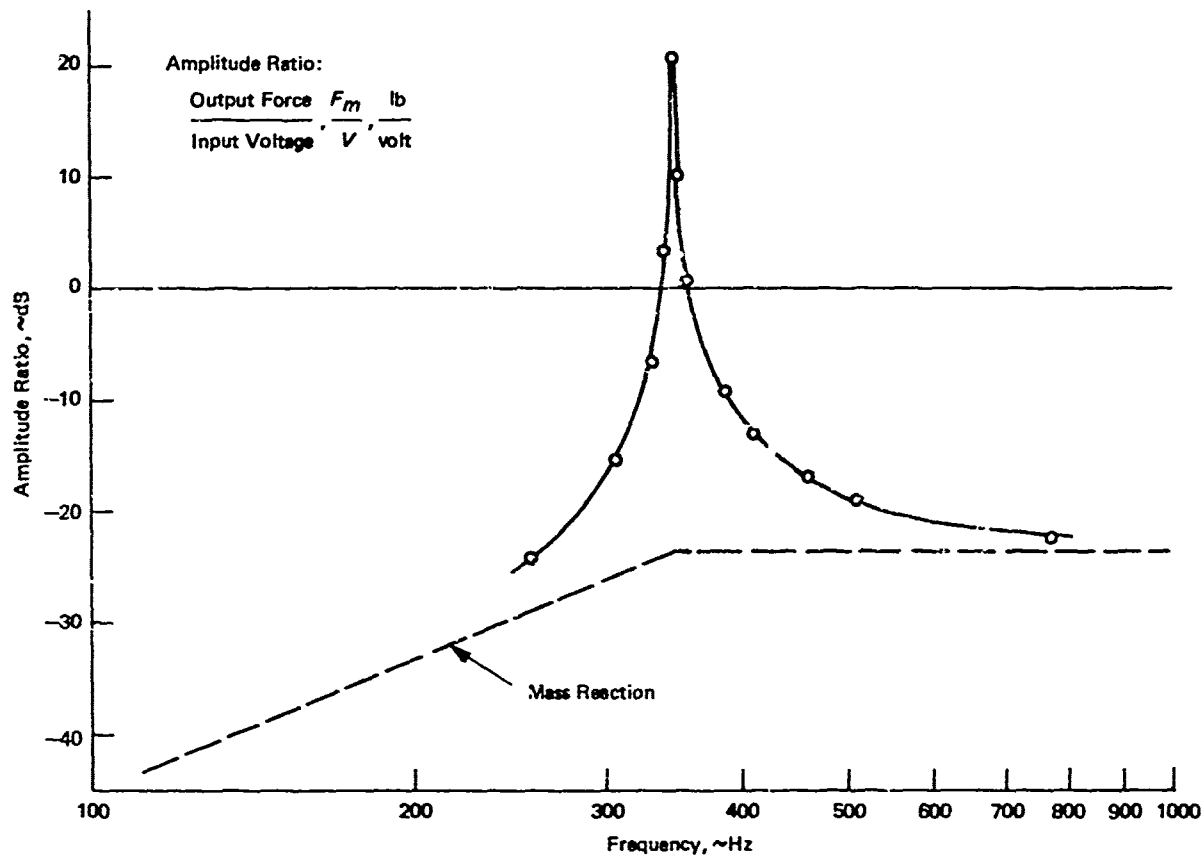


FIGURE 5. FREQUENCY RESPONSE RADC TRANSDUCER INFINITELY STIFF LOAD (BACK-TO-BACK)

voltage over the frequency range of 250 to 800 Hz. Output force was determined as the product of mechanical resonator mass and the measured acceleration of the mass. Input drive voltage and frequency were measured, and, in addition, an accelerometer was mounted on the interface plate between the two transducers to monitor the quality of the dynamic match between the two units. This signal was found to be more than 40 dB less than the mass accelerations, and so the match appeared adequate for purposes here. This was further verified by the fact that the measured accelerations on each of the two masses were very nearly equal. With calculated values of  $L$  and  $C_r$ , and with already measured values of  $hC_o$  and  $C_c$ , the results obtained from Figure 5 were sufficient to determine values for  $C$  and  $(R + R_p)$  [see Eqs. (5) and (6) with  $R_p = \infty$  and  $C_p = 0$ ].  $R$  and  $R_p$  were then apportioned to the two springs in inverse proportion to the respective spring rates.

#### c. Tabulated Numerical Values

From the preceding laboratory tests and by calculation of the more certain quantities, the following numerical values were assigned for the elements shown in the equivalent circuit model of Figure 3. The values have been averaged for each of the two RADC transducers and are given in both MKS and convenient engineering units.

$nC_o = 0.0132 \mu\text{F}$	
$hC_o = 6.2 \text{ A sec/m}$	$= 0.158 \text{ A sec/in.}$
$hC_o = 6.2 \text{ N/V}$	$= 1.4 \text{ lb/V}$
$C_c = 2.12 \times 10^{-10} \text{ m/N}$	$= 0.037 \times 10^{-6} \text{ in./lb}$
$C_r = 233 \times 10^{-10} \text{ m/N}$	$= 4.07 \times 10^{-6} \text{ in./lb}$
$C = 42.8 \times 10^{-10} \text{ m/N}$	$= 0.748 \times 10^{-6} \text{ in./lb}$
$R = 690 \text{ N sec/in.}$	$= 3.94 \text{ lb sec/in.}$
$R_r = 126 \text{ N sec/m}$	$= 0.72 \text{ lb sec/in.}$
$L = 56.5 \text{ N sec}^2/\text{m}$	$= 0.323 \text{ lb sec}^2/\text{in.}$

If one chooses to employ the simplified equivalent circuit model of Figure 4 and the related equations, the following values are used:

$nC_o = 0.0132 \mu\text{F}$	
$hC_o = 6.2 \text{ A sec/m}$	$= 0.158 \text{ A sec/in.}$
$C_c = 2.12 \times 10^{-10} \text{ m/N}$	$= 0.037 \times 10^{-6} \text{ in./lb}$
$L = 56.5 \text{ N sec}^2/\text{m}$	$= 0.323 \text{ lb sec}^2/\text{in.}$
$C^* = 35.5 \times 10^{-10} \text{ m/N}$	$= 0.62 \times 10^{-6} \text{ in./lb}$
$R^* = 19.4 \times 10^6 \text{ N sec/m}$	$= 111,000 \text{ lb sec/in.}$
$K = 0.837$	

#### d. Performance Calculations

Using the numerical values cited above, performance calculations were made, and the results are shown plotted in Figures 6 and 7. The first curve presents the radiated power output for various drive voltages as a function of the equivalent parallel seismic load resistance,  $R_p$ , while the second curve indicates the variation of power conversion efficiency and information bandwidth with this same parameter. The curves were calculated for an assumed nominal resonant frequency of 334 Hz. Several interesting points are seen at once by examination of these curves. First, the power radiating capability of the transducer is strongly load dependent and increases with increasing  $R_p$  up to the matched load point. Higher values of  $R_p$  are associated with hard, competent rock.

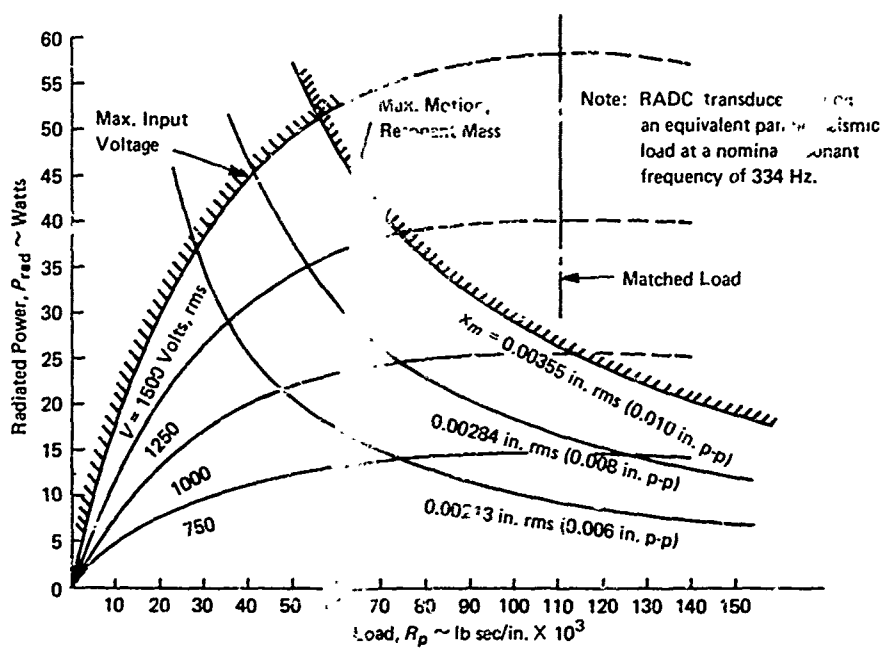


FIGURE 6. RADC TRANSDUCER, RADIATED POWER

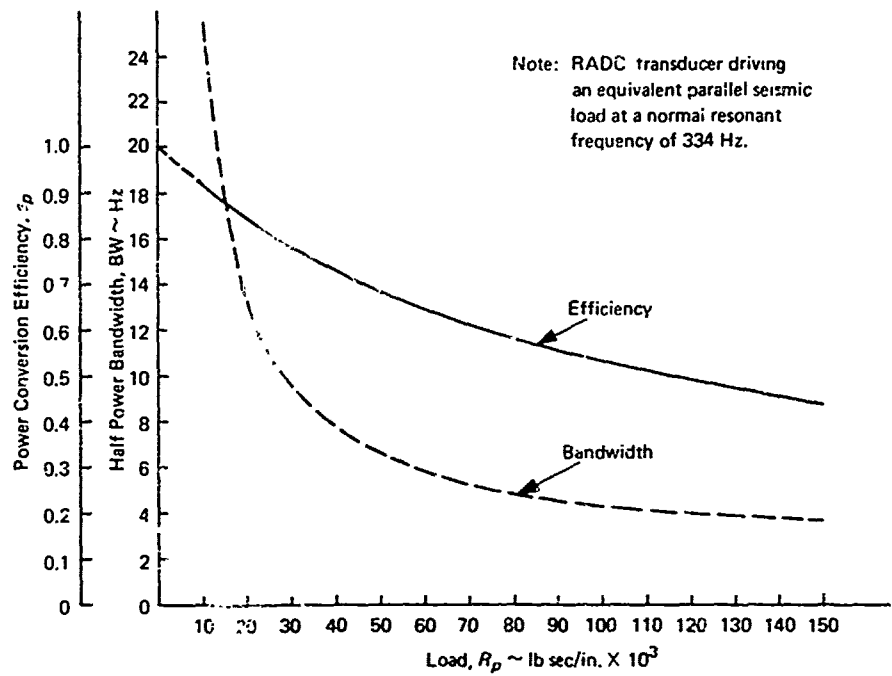
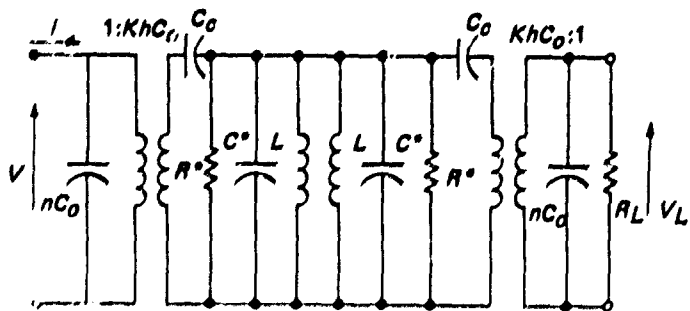


FIGURE 7. RADC TRANSDUCER, EFFICIENCY AND BANDWIDTH

Consequently, the unit was clearly designed for operation into such media. Maximum power operation at the matched load point cannot, in fact, be realized because of motional limits on the excursion of the resonant mass; such limits were probably in turn derived from maximum operating stress limits. Rock media exhibiting such a high value of  $R_p = 111,000$  lb in./sec are probably nonexistent in any event, and so actual maximum power operation in the vicinity of  $R_p = 40,000$  to 60,000 lb sec/in. is more realistic. Because of narrow practical limits, there was no attempt here to investigate impedance matching horns beyond that of providing the 6-in.-diameter drive plate in lieu of using the 3-in.-diameter transducer base. This appeared to be a step in the right direction from the standpoint of impedance matching. Second, the transducer does indicate high-power conversion efficiencies in the range of 0.8 or so for typical hard rock media encountered in field experiments to be described later. And third, the device exhibits a very limited information bandwidth of the order of 10 to 12 Hz. The narrow bandwidth is not surprising when the high Q nature of the unit is considered. Moreover, the high Q characteristic is not incidental; it has, in fact, been employed to multiply the reaction of the mass element (125 lb weight) acting against the outer surface of the crystal stack and thus facilitating the radiation of power into the seismic medium. To make the unit broadbanded with the same power radiating capability would require the use of a reaction mass (non-resonant) weighing 10,000 lb or more. Not only is this an absurdity, but such a mass of steel or lead would doubtless corrupt the frequency range of interest with a whole spectrum of internal propagational modes; i.e., it would not appear as a lumped reactive mass element at the crystal stack face. Another solution would be to load both faces of the crystal stack against the rock medium by mounting the unit in a crevice between two rock faces, for example; again, this would not be too practical an approach for general use.

#### *a. Power Transfer (Motor-Generator Mode)*

Since little power was consumed in the back-to-back tests reported previously, it was decided to attempt to transfer power in a motor-generator mode in which the two transducers were mounted back-to-back with the drive applied to one transducer and the other loaded with an electrical resistor across the crystal terminals. It was thought that, in this way, maximum power radiating capabilities could be determined as well as efficiency of power conversion. However, these tests did not prove particularly satisfying for two reasons. First, extending the simplified equivalent circuit of Figure 4 to represent the motor-generator mode, there results the following equivalent circuit:



The input power is given by  $Vi \cos \theta$  where  $\theta$  is the phase angle while the output power is  $|V_L|^2/R_L$  where all quantities are given in rms units. The problem arises in that this circuit does not behave simply as a single transducer driving into a seismic load as might be suspected by inspection. For one thing, the Q at resonance is lower, and it might be expected that internal losses would be higher by a factor of two. Also the electrical load,  $R_L$ , is not linearly related to the seismic load element,  $R_p$ , and in fact, it is not possible to simulate a seismic load less than 65,000 lb sec/inch. In addition, it was found that, because of the nonlinear behavior of the transducer, the current wave shape was not sufficiently sinusoidal to permit accurate phase angle measurements for purposes of calculating input power. Despite these conceptual and practical difficulties, tests were run in which output power as high as 25 W was measured with input power of perhaps 50 W corresponding to an equivalent  $R_p$  of about 65,000 lb sec/inch. By interpretation, assuming the losses were twice as high in this mode, this would correspond to an efficiency of about 0.67 for a single transducer operating into the same seismic load. In Figure 7, it is seen that the correct efficiency for  $R_p = 65,000$  lb sec/in. is 0.63. Consequently, this exercise did serve to corroborate previous results in general, as well as to demonstrate the transfer of a reasonable amount of power.

#### *f. Transducer Nonlinearity*

The problem of nonlinear behavior of the transducer was just mentioned; thus, it seems in order to further discuss this matter since the ramifications of this difficulty were felt throughout the remainder of this work. The initial symptoms of this nonlinearity were (1) a definite downshift in the transducer resonant frequency with increasing output level, making it extremely difficult because of the high Q to tune onto resonance with an oscillator and (2) the observed nonsinusoidal departures of the drive current wave shape. Later, when the drive plate was instrumented with accelerometers, the nonsinusoidal wave shape was noted again. In all cases, the nonlinearity increased with output level. Interestingly, the measured acceleration of the resonant mass did not deviate as markedly from sinusoidal shape, apparently because of the filtering effect of the high Q resonator. In diagnosing this problem, it was found that the nonlinearity occurred only on the half cycle when the operating forces were in a direction to relieve the load applied by the preload rod. The main spring in effect becomes softer as the total load is decreased. Tightening of the preload rod improved the nonlinearity, but this effect could not be pursued because of the already high working stresses in the rod (SAE 4140, heat treated). As noted earlier, the crystal stack, main spring, and mass are all coupled solely through this preload, and it is believed that this is a design deficiency from which the nonlinearity originates. This could be remedied through proper redesign. At any rate, the problem did affect all succeeding tests where drive plate acceleration data were measured for the purpose of calculating radiated power and driving point impedance, since it was not possible to measure phase angle with any reasonable degree of precision.

#### *g. Driving Concrete Pier Load*

To provide some foreknowledge of transducer performance operating into a seismic load and to provide, simultaneously, a test-bed for finalizing the experimental equipment design, the transducer was attached to the concrete floor in the laboratory, directly above a heavy concrete floor beam and an 18-in.-diameter pier extending some 36 ft down to limestone layers in the earth. A heavy concrete anchor bolt imbedded in the floor was drilled and tapped to accept the preload rod for purposes of positive attachment. A 5-in.-diameter drive plate was employed in this instance, principally to provide a pad for mounting an accelerometer. Thus, the transducer was affixed to the concrete at a single-point tie using the preload rod. From this experience, during which the crystal stack on one of the transducers was fractured because of inadvertent loss of crystal preload during

the mounting procedure, it was decided to employ a different mounting technique for the field experiments. A 6-in.-diameter drive plate was designed, providing a means for anchoring the preload rod independently of attachment to the rock medium. This in turn required the use of three smaller anchor bolts to attach the transducer to the rock. By this method, the transducer assembly was always under preload and not subject to accidental damage during handling, mounting, etc.

Both RADC transducers were operated into the concrete pier load. A typical frequency response wave for one of the units is presented in Figure 8. This gives the amplitude ratio of output force to drive voltage, and the loss in Q due to loading is seen by comparing this to the infinite load frequency response of Figure 5. Note also the lower resonant frequency. The driving point

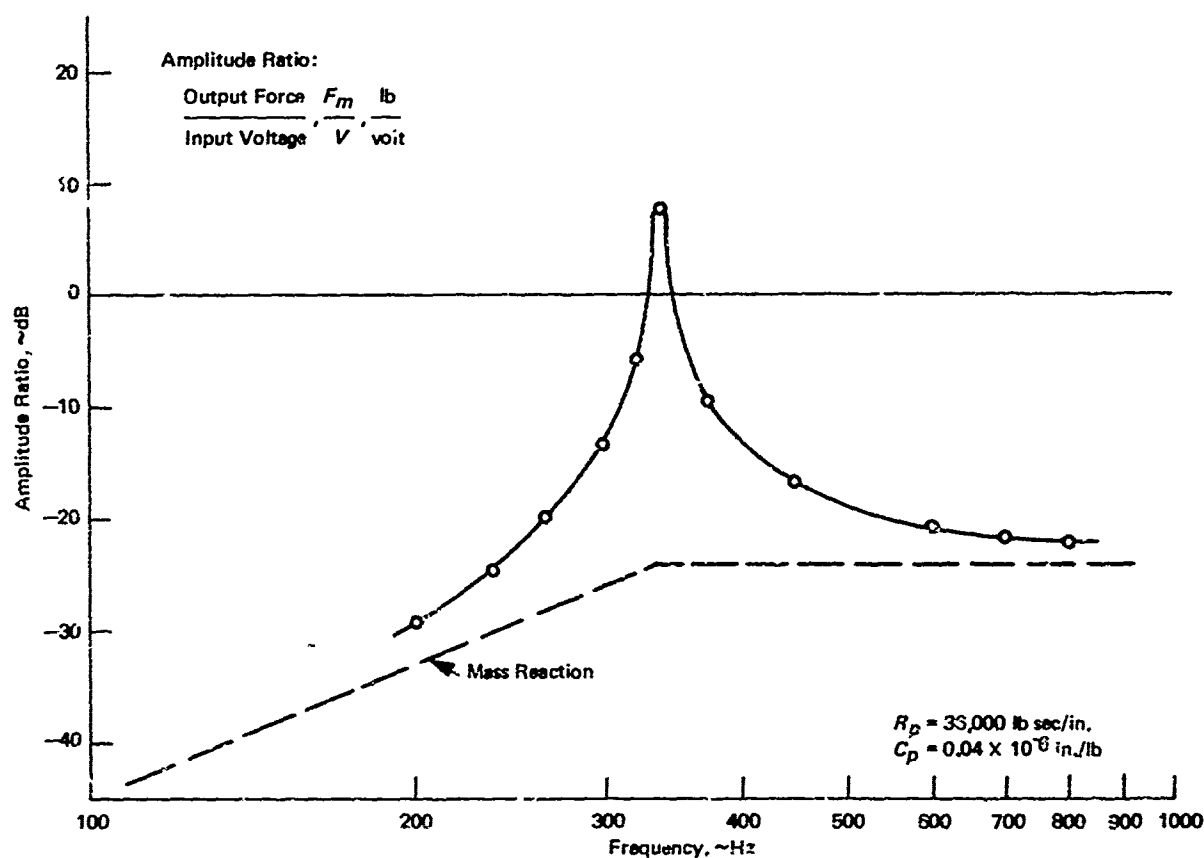


FIGURE 8. FREQUENCY RESPONSE RADC TRANSDUCER CONCRETE PIER LOAD

impedance at the transducer-concrete floor interface was calculated from measured values of interface force,  $F_m$ , and interface acceleration (converted to velocity). This required phase angle measurement, and precision was therefore limited by nonlinear behavior as discussed above, although these measurements were made at low drive levels with correspondingly reduced nonlinear effects. The average value of driving point impedance,  $Z_g$ , determined from a number of individual measurements was, at a resonant frequency of 337 Hz:

$$Z_g = 4000 - j 11,500 \text{ lb sec/in.}$$

This corresponds to

$$R_p = 37,000 \text{ lb sec/in.}$$

$$C_p = 0.037 \times 10^{-6} \text{ in./lb}$$

Moreover, it was found that the parallel representation with the values given here was quite good for this concrete pier load over the range of 200 to 800 Hz. Plugging these values of  $R_p$  and  $C_p$  back into Eqs. (5) and (6), or alternatively Eqs. (12) and (13), yields values of  $F_m/V$  and  $\omega$  at resonance very close to those given in the experimental data. This further confirms the form of the mathematical model and the numerical values previously determined.

Power radiated into the load is given by  $F_m v \cos \phi$  where  $v$  is the velocity of the drive plate and  $\phi$  is the phase angle between  $F_m$  and  $v$ .  $F_m$  and  $v$  are given in rms units. Radiated power was calculated from the experimental data using this expression and compared to the radiated power given in Figure 6 using  $R_p = 37,000 \text{ lb sec/in.}$  and the drive voltage level. These comparisons were not consistent over a number of separate measurements evidently because of the lack of precision in phase angle measurement. It was concluded that the best estimate would result by using Figure 6 with the measured value of  $R_p$ . From this it is seen that power of about 43 W was radiated into the concrete pier for a drive voltage of 1500 V rms. This same technique was later used in the field experiments to estimate radiated power.

The electrical input impedance,  $Z_i$ , at the crystal stack terminals was found, for the same condition of resonance as above, to be

$$Z_i = 9750 - j 16,900 \Omega$$

The corresponding input power for  $V = 1500 \text{ V rms}$  is 57.5 W, which yields a power conversion efficiency of 0.75, in very close agreement with the result given in Figure 6. Note also that the drive force,  $F_m$ , was 3810 lb rms (5390 lb peak).

These concrete pier tests also facilitated the completion of the experimental equipment buildup, the final form of which is described in the next section.

## SECTION III

### EXPERIMENTAL EQUIPMENT

#### 1. GENERAL ARRANGEMENT

Development of instrumentation and equipment was not one of the contract objectives. However, a buildup of equipment was required to perform the various laboratory and field tests, and it might be instructive to review briefly those arrangements. For the field experiments, two general types of tests were planned:

- (1) Local transmitter tests employing CW excitation and instrumentation to measure resonant mass and drive plate accelerations, from which, together with other measured data, the driving point impedance,  $Z_g$ , could be calculated. This in turn permitted an estimate of radiated power, conversion efficiency, force output, and bandwidth at the transmitter installation.
- (2) Seismic propagation and communications experiments, employing one RADC transducer as the transmitter and the other as a receiver, with operation in a gated pulse mode. Because of the narrow information bandwidth and poor control of the transducer-installed resonant frequency, it appeared that little would be gained by consideration of modulation methods other than simple pulse width or pulse code. Thus, it was planned to transmit in the gated pulse mode with capability of varying the on-time of the pulse. Means for remote triggering of the transmitter from the receiver site, via wire line, was provided so as to facilitate propagation velocity measurements. Provision was also made to employ a sensitive accelerometer as a seismic receiving unit.

Block diagrams showing the equipment arrangements for the local transmitter tests and for the transmitter and receiver unit propagation tests are presented in Figures 9, 10, and 11, respectively. Corresponding photographs of the equipment packages are presented in Figures 12, 13, and 14, respectively. Standard laboratory instrumentation was employed wherever possible though this did result in sporadic operational difficulties in the iron mine tests due to the high humidity environment. Special equipment design and fabrication were required in only two areas: (1) the high-voltage drive transformer and (2) the unit identified as the control circuit. A description of these two items follows.

#### 2. DRIVE TRANSFORMER

This unit was required to match the dual, class A, tube-type audio power amplifier to the transducer crystal stack. The dual amplifiers were connected to provide an output impedance of  $32 \Omega$  and a peak voltage of about 57 V rms, while delivering a maximum power of 100 W. Input power required from the 110-VAC line was 200 W. The crystal stack, on the other hand, required that 1500 V rms be delivered into an impedance of the order of  $(9750 - j 16,900 \Omega)$  at the nominal resonant frequency of about 335 Hz. A special transformer was ordered with a 27:1 step-up ratio, and a 10-henry choke was connected across the secondary to correct the poor power factor of the load. This resulted in a fairly good match with the load appearing as a nearly resistive load of about 39,000  $\Omega$ .

Note: All equipment battery powered  
except as noted.

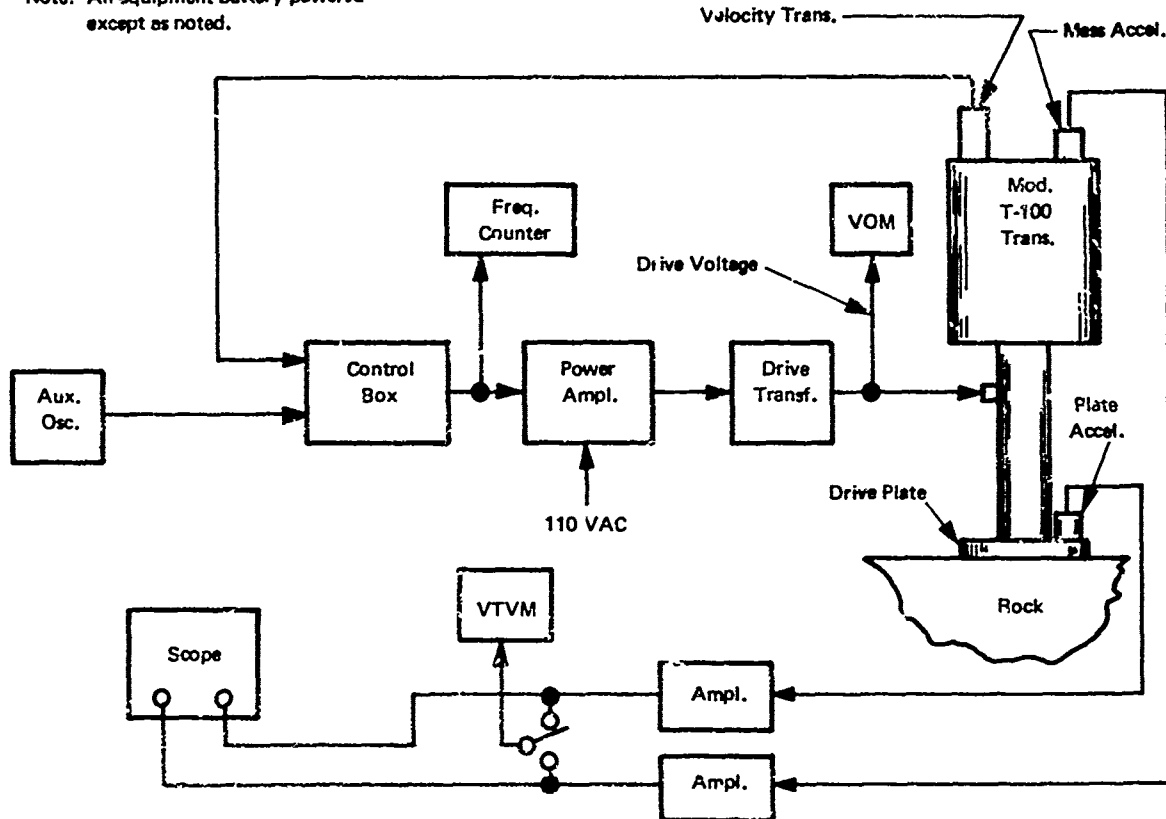


FIGURE 9. LOCAL TRANSMITTER TEST ARRANGEMENT

Note: All equipment battery powered  
except as noted.

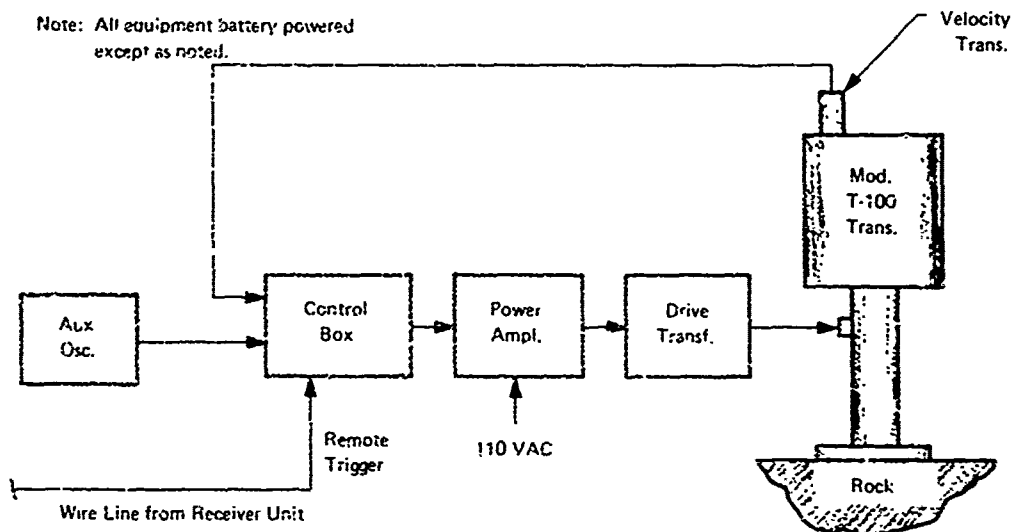


FIGURE 10. TRANSMITTER UNIT, PROPAGATION TESTS

Note: All equipment battery powered.

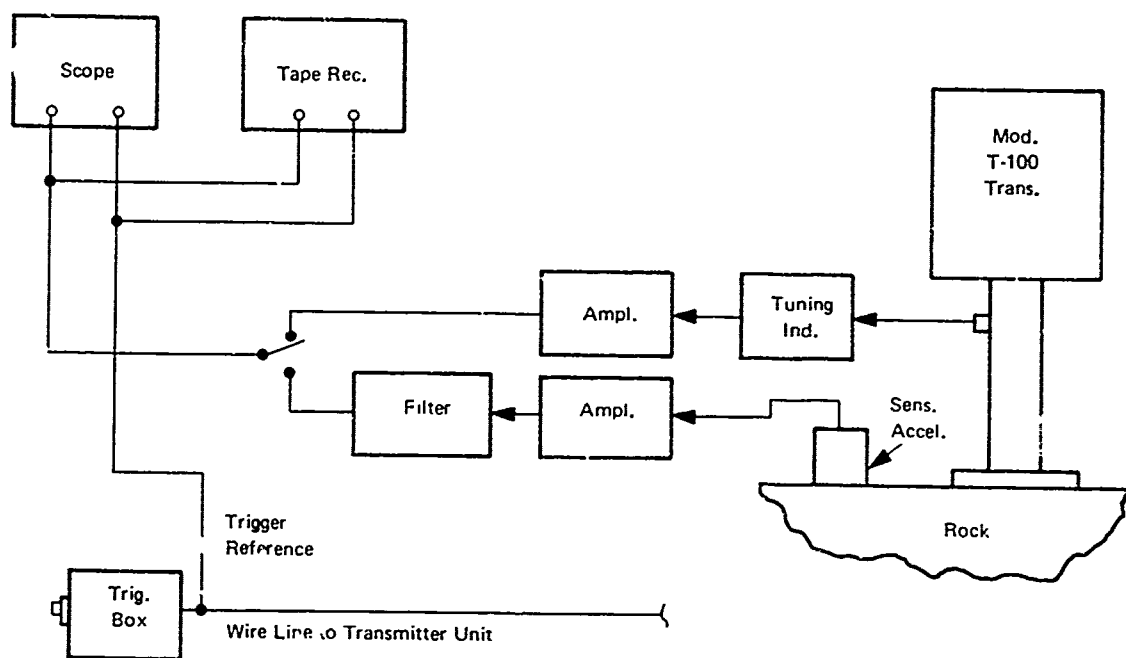


FIGURE 11. RECEIVER UNIT, PROPAGATION TESTS

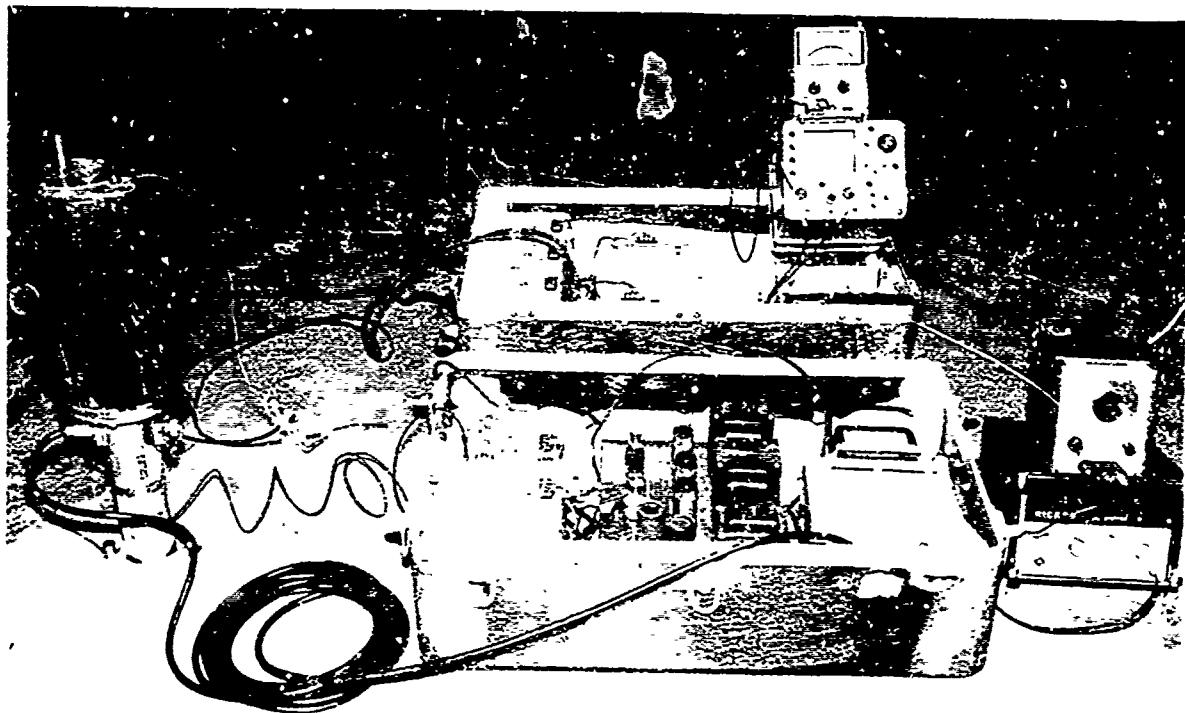


FIGURE 12. LOCAL TRANSMITTER TEST EQUIPMENT

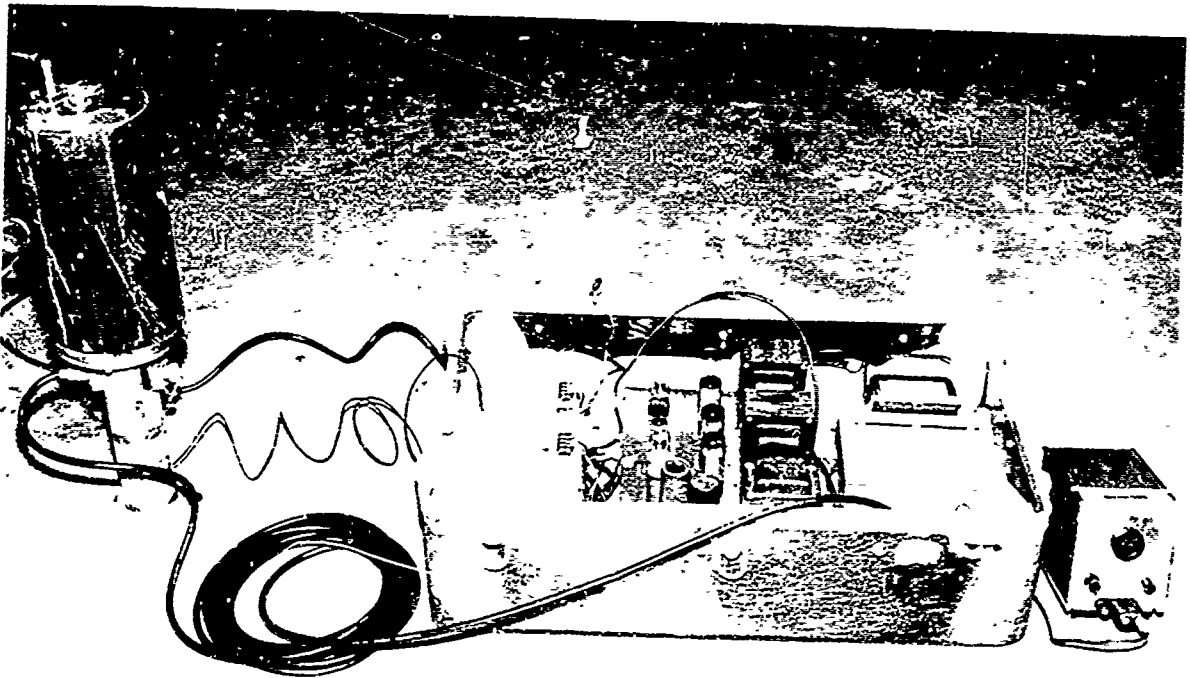


FIGURE 13. TRANSMITTER UNIT TEST EQUIPMENT

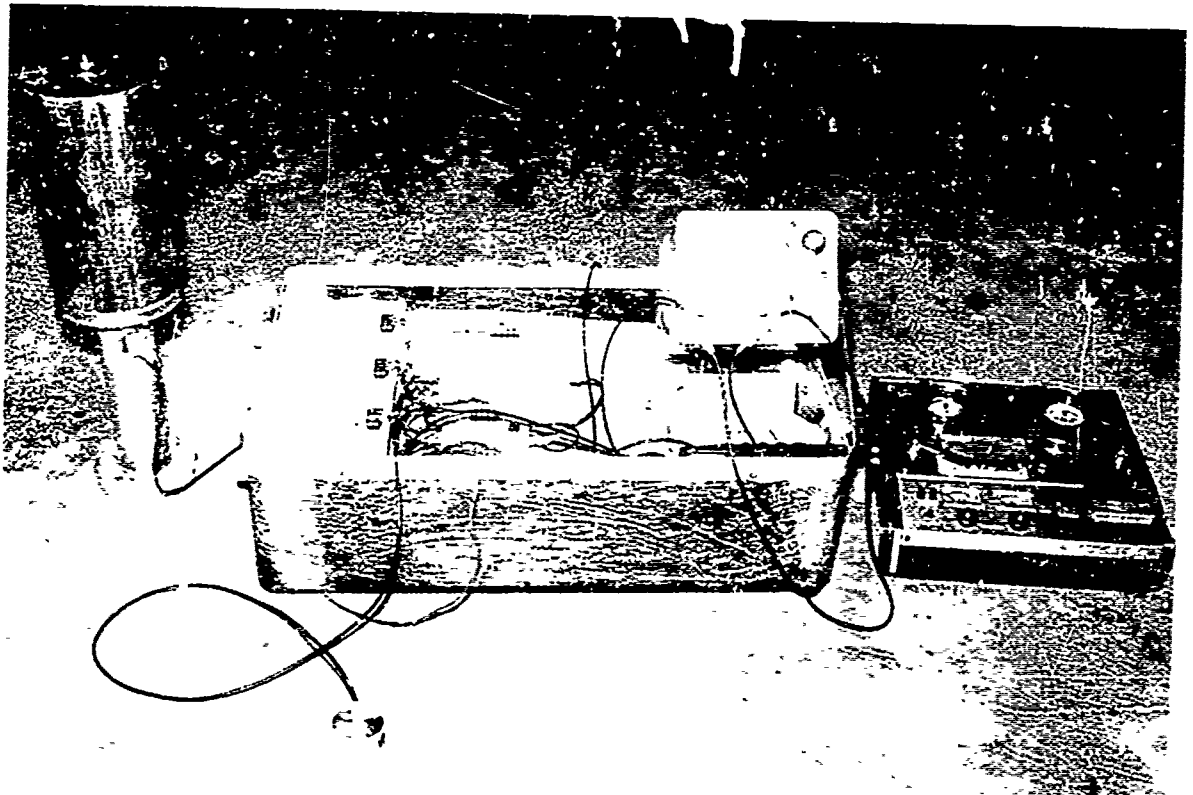


FIGURE 14. RECEIVER UNIT TEST EQUIPMENT

### 3. CONTROL CIRCUIT

In the laboratory tests, there was considerable difficulty in tuning the transducer to resonance. Further, since the resonance is shifted by the seismic load reactance at each installation, there could be no predetermined drive frequency. Accordingly, it was decided to close the loop around the transducer and allow it to oscillate at its own self-resonance and thus generate maximum power radiating capability. This was accomplished by installing a velocity sensor on the RADC transducer resonant mass and feeding this signal back to the drive amplifier in positive feedback manner. The control circuit, shown schematically in Figure 15, was devised to accomplish this purpose. Since it

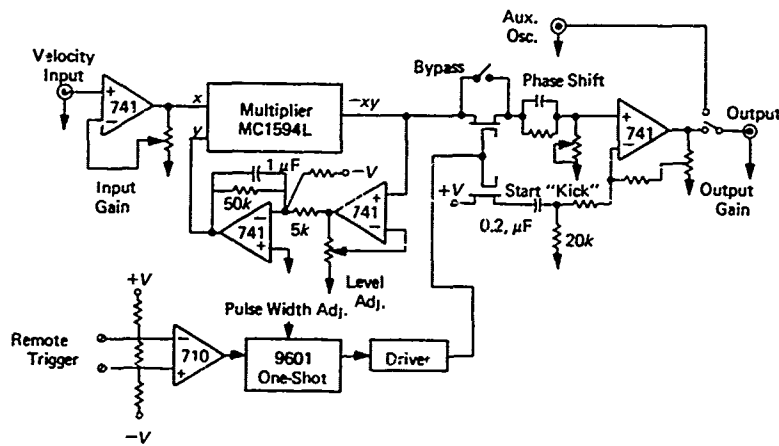


FIGURE 15. CONTROL BOX—SIMPLIFIED SCHEMATIC

was desired to operate the source transducer in a gated pulse mode, provisions were made to close and open the feedback loop with a solid-state switch controlled by a one-shot. The one-shot in turn was fired by the remote trigger wire line. Further refinements were incorporated in the circuit to permit very fast turn-on of the transmitter limited only by the inherent Q of the mechanical resonance. One of these consisted of a variable gain element, a multiplier, which was configured to provide very high loop gain at the initiation of a pulse but with gain rapidly decreased by the buildup of the average loop drive level. Thus, the final drive level was controlled but without inhibiting the initial buildup time. Also a start "kick" pulse was provided to bring the velocity sensor signal up to the threshold of response. The phase shift adjustment was found useful in permitting resonance to occur directly at the point of maximum amplitude excursion. The control circuit was successfully employed in the concrete pier experiments and later in the field; however, each separate installation required appropriate tune-up of gains, phase shift, etc.

## SECTION IV

### LIMESTONE QUARRY EXPERIMENTS

#### 1. TEST SITE DESCRIPTION

Seismic communications tests were initiated in an open-formation limestone quarry about 35 mi northeast of San Antonio near New Braunfels, Texas. The quarry is owned and operated by U.S. Gypsum Co. These tests were performed over a period covering the first 2 weeks in April 1972. A plan view of the test site and a typical cross section are presented in Figure 16. The limestone is identified as Edwards Limestone and is considered a relatively hard, competent rock generally, though varying in places to relatively soft and spongy in character. As seen in the figure, one receiver

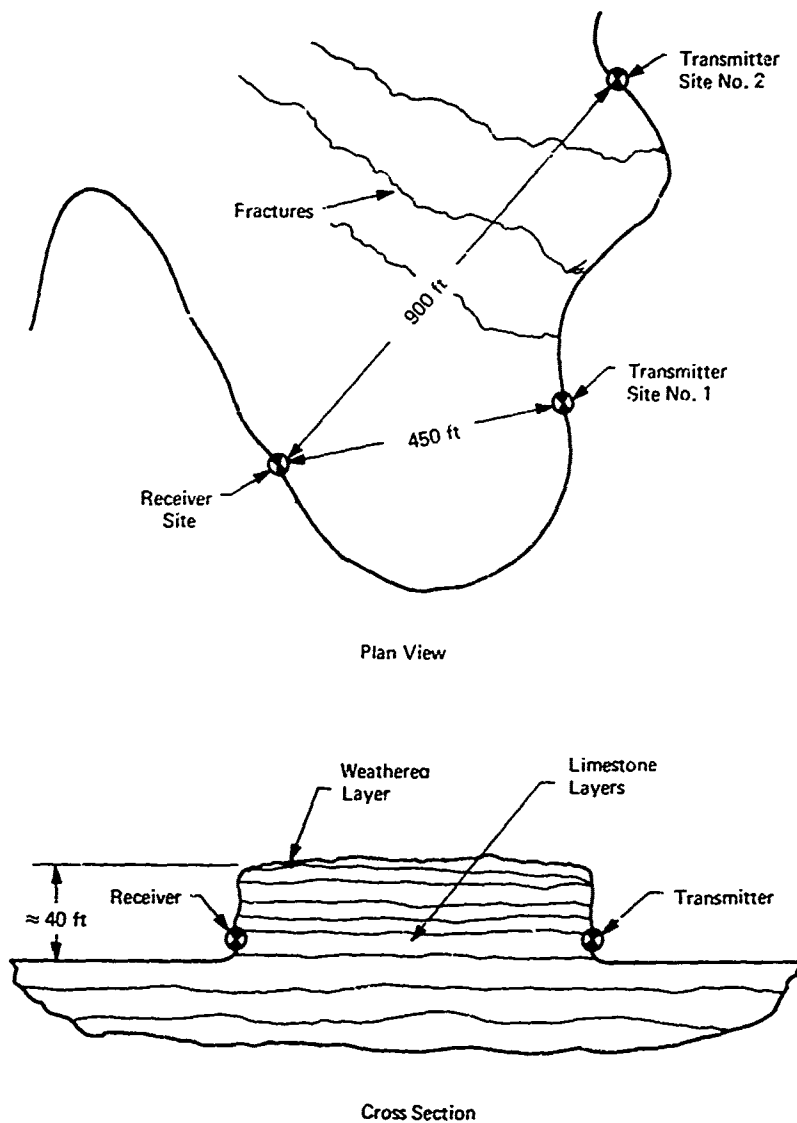


FIGURE 16. LIMESTONE QUARRY TEST SITE

site was employed, while the transmitter was installed at two different sites. The RADC transducer installation at the receiver site is shown in Figure 17, while Figure 18 is a photograph of a typical mounting "pad". The anchor bolts are of the split-ring type and are 3/4 in. in diameter and 6 in.

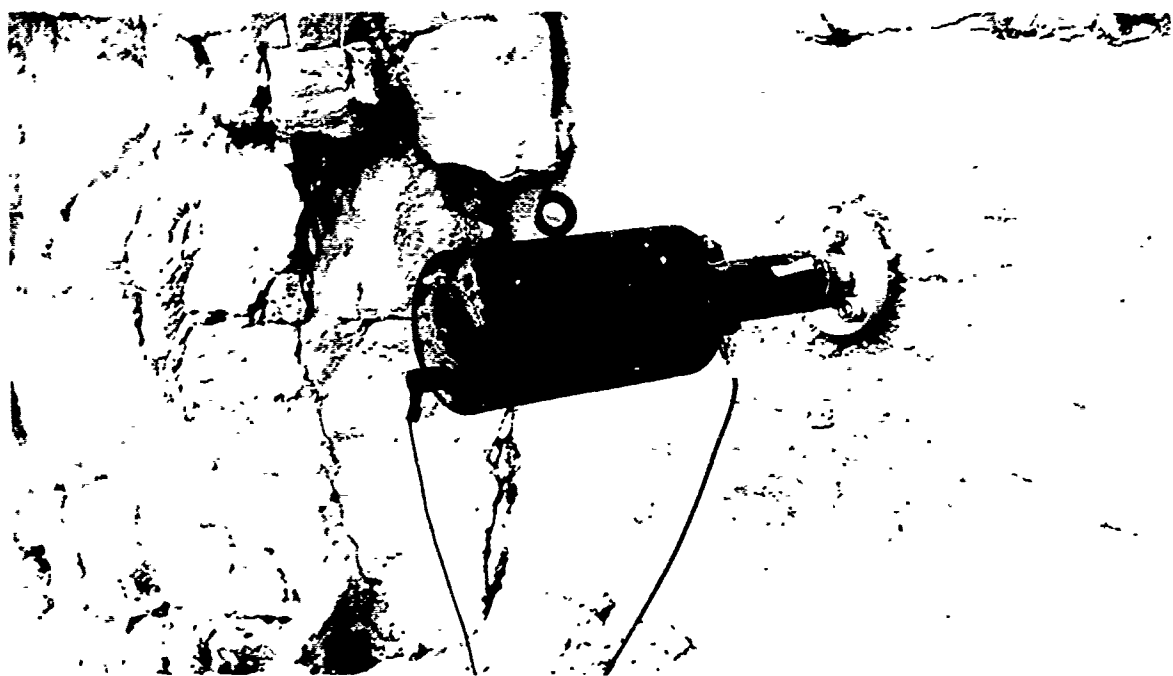


FIGURE 17. LIMESTONE QUARRY—RECEIVER TRANSDUCER INSTALLATION

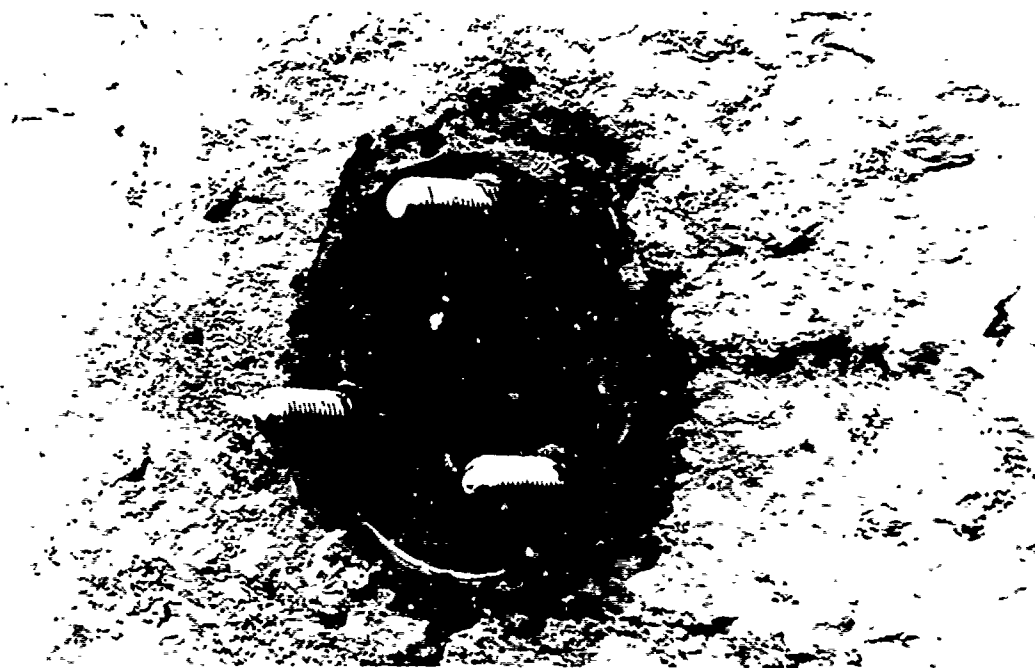


FIGURE 18. TYPICAL TRANSDUCER MOUNTING PAD

long. Quick-setting grout was applied under the drive plate to provide uniform coupling to the rock across the full face of the plate. Figure 19 is a photograph of the transducer installation at transmitter site No. 1, showing plainly the layered limestone structure. The other two transducer installations appeared very similar to this, and, in each case, the transducer was affixed to what was believed to be the identical limestone layer. At each site, an attempt was made to select an attachment point on the rock that appeared to be free from surface cracks and that evidenced hard, competent character in response to hammer blows.



FIGURE 19. LIMESTONE QUARRY--TRANSMITTER SITE NO. 1

## 2. TEST RESULTS

### a. Propagation Path: 450 Ft

So-called "local transmitter" tests were performed at both the initial transducer installations, identified later as the receiver site, and at transmitter site No. 1. It was found that little power could be radiated at the receiver site. This was corroborated by driving point impedance measurements yielding

$$R_p = 8370 \text{ lb sec/in.}$$
$$C_p = 0.165 \times 10^{-6} \text{ in./lb}$$

at a resonant frequency of 317 Hz. Measured force,  $F_m$ , was 637 lb rms at maximum drive voltage capability of 950 V rms. The radiated power worked out to be about 5 W. At transmitter site No. 1, the results were much superior, with driving point impedance measurements giving

$$R_p = 17,800 \text{ lb sec/in.}$$
$$C_p = 0.143 \times 10^{-6} \text{ in./lb}$$

at a resonant frequency of 315 Hz. Measured force was 1975 lb rms at 1500 V rms, and radiated power was about 25 W. No explanation for this discrepancy in driving point impedance at different points in the same rock layer was found. However, it is surmised that subsurface cracks in the rock formation, perhaps even several feet below the exposed surface, could well result in variations of this magnitude. At any rate, because of these findings, signal transmissions were made only from the latter site and received at the former, thus the identifications as given above.

The transmitter unit was triggered by wire line from the receiver site, and a large number of pulse signals were recorded with signal-to-noise ratios greater than 40 dB despite the presence of heavy quarry machinery operating about 200 yd away. Actually, acoustic coupling due to near aircraft flyovers and close human voices was more of a problem. Figure 20 presents typical recorded signals. The upper trace is the trigger; the second is the acceleration of the transmitter unit drive plate (the seismic input signal in this case); and the third is the signal received by the receiver unit. The input gated pulse is about 0.14 sec long and exhibits essentially first-order exponential rise and decay as determined by the Q of system resonance. (Note the start "kick" at the trigger point.) The received signal exhibits second-order-type onset just as it might be expected for a first-order system to respond to a first-order signal input. Note that the tail trails off considerably.

The velocity of propagation of this signal was found by subtracting the time for the input signal to reach 63 percent of final value on the onset from the time required for the received signal to reach 27 percent of final value. This is the correct relationship if the two first-order time constants are equal. This time difference was 0.05 sec. The propagation velocity for the 450-ft path was thus 9000 ft/sec. Since this velocity appeared slow for the compressional wave velocity in hard, competent limestone, impulse tests were performed to shed some light on propagational velocities in this seismic transmission path. Impulses were generated by sledge hammer blows on the rock face within a few feet of the transmitter unit installation. The drive plate accelerometer signal was again recorded as the input signal, and received signals were recorded from the RADC transducer and from a sensitive accelerometer at the receiver site. Typical results of these tests are shown in Figure 21. The upper trace is the seismic input signal; the second is the received signal from the RADC transducer; and the third is the received signal from the sensitive accelerometer. The RADC transducer

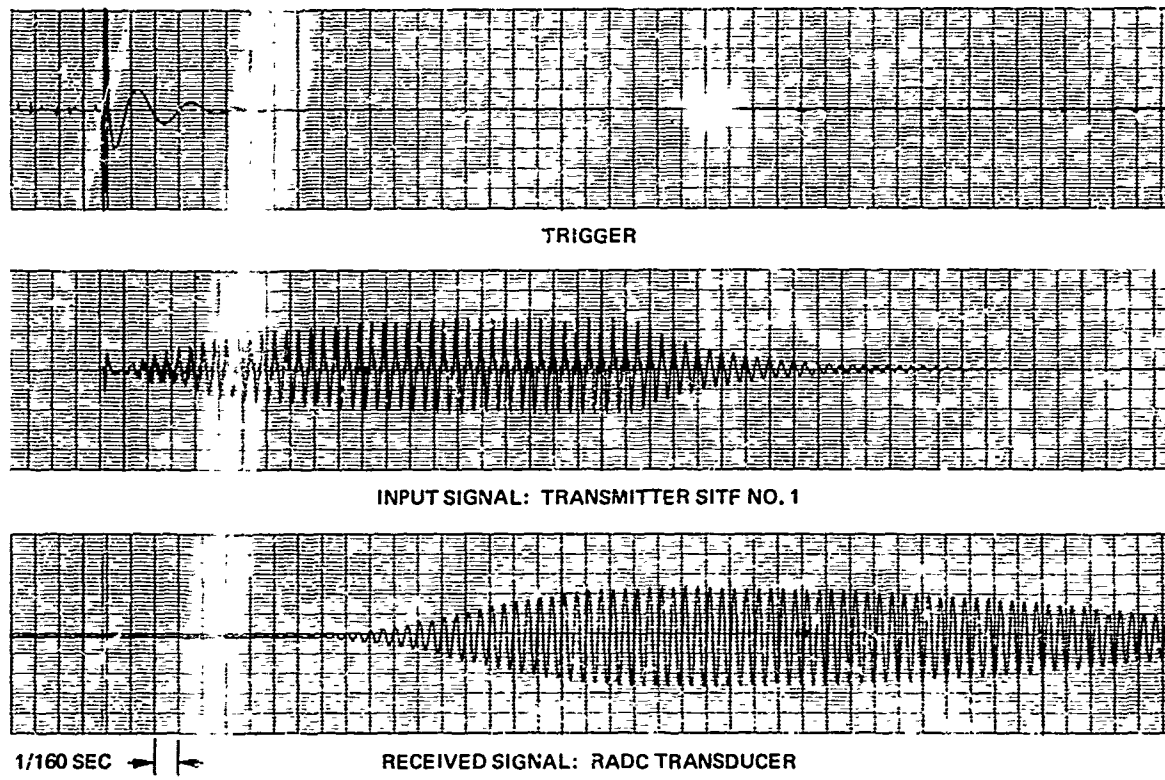


FIGURE 20. LIMESTONE QUARRY-TYPICAL TRANSMISSION (450-Ft Path)

is of course narrow band with a bandwidth of perhaps 20 Hz centered about 317 Hz. The sensitive accelerometer on the hand is broadband over a wide range leading up to a resonance around 800 Hz. The first arrival on both receiving units is seen to come at about 0.025 sec from the initial onset of the impulse. This gives a propagation velocity of 18,000 ft/sec, which is a reasonable value for the compressional wave velocity in the medium. This confirms that compressional wave propagation was insignificant in the RADC transducer gated pulse tests and that the dominant mode might have been shear body waves, surface waves, or some other form of more complex waves as discussed by Owen.<sup>(1)</sup> Miller and Pursey<sup>(10)</sup> show that, for a source driving into an isotropic half space, the energy is partitioned approximately as follows:

compressional wave: 7 percent  
 shear wave: 26 percent  
 surface wave: 66 percent

This indicates that surface wave propagation, at least under the ideal conditions assumed, soaks up most of the energy available. Accordingly, it is probably not too inaccurate to assume that the major propagational mode encountered here was surface wave, with the wave simply propagating over the open formation with a wavelength of about 30 ft.

Since the main applications of interest here preclude surface wave propagation, simply from topological considerations, it was concluded that further tests in an actual mine environment would be necessary to ascertain the feasibility of the subject seismic communications method.

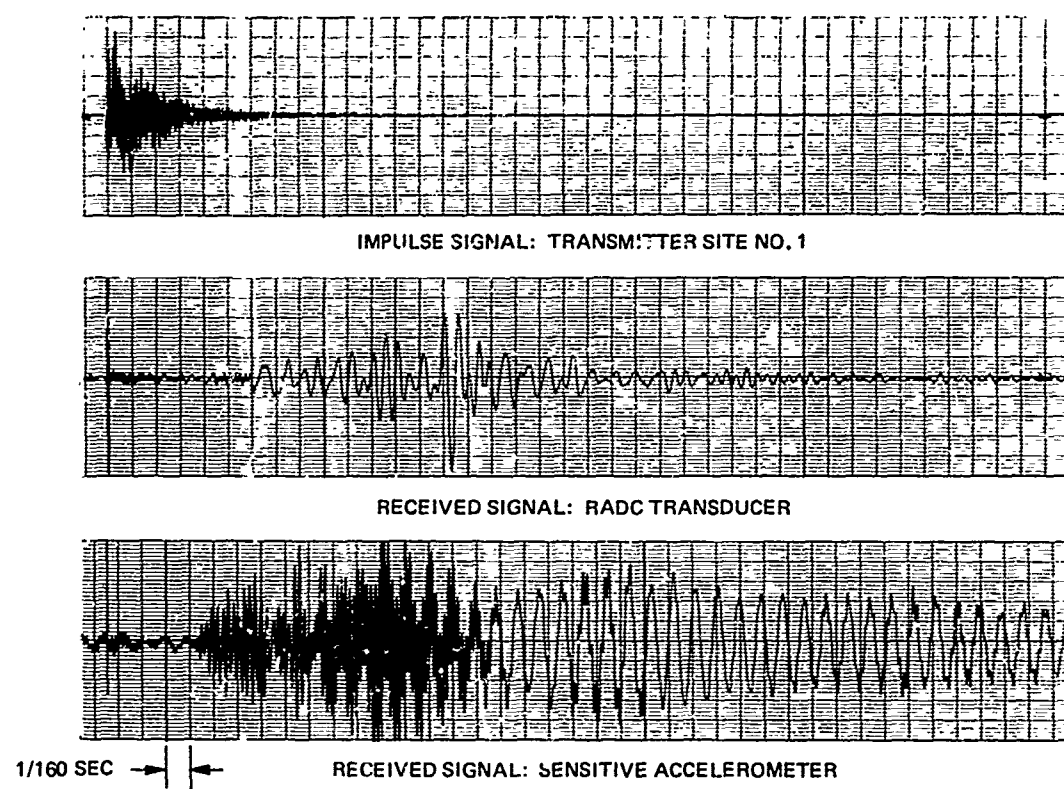


FIGURE 21. LIMESTONE QUARRY-IMPULSE RESPONSE (450-Ft Path)

Accordingly, arrangements were made to mount an experimental effort in an operating mine, and these efforts and the results achieved are reported in the next section. However, to gain some further experimental data in the quarry, transmission over a longer distance was attempted with results reported next.

*b. Propagation Path: 900 Ft*

One RADC transducer was moved to transmitter site No. 2 as shown in Figure 16, while the receiver unit was retained at the original location. As before, "local transmitter" tests were performed with the driving point impedance measurements giving

$$R_p = 9100 \text{ lb sec/in.}$$

$$C_p = 0.103 \times 10^{-6} \text{ in./lb}$$

at a resonant frequency of 320 Hz. Measured force was 1020 lb rms at a maximum drive voltage capability of 1375 V rms. Radiated power was about 14 W. Again, as at the receiver site, this proved to be a relatively "soft" coupling. The loss in radiated power, the doubling of the length of the transmission path, and the existence of what appeared to be large fractures across the transmission path all combined to the extent that no signal was received above the noise level for any of several types of receivers. Nor was it possible to receive impulse signals generated by sledge hammer blows. Thus, some idea of potential limitations to this method of seismic communications was made evident.

## SECTION V

### IRON MINE EXPERIMENTS

#### 1. GENERAL DESCRIPTION AND ARRANGEMENTS

Arrangements were made with the Meramec Mining Co. to perform a series of experiments in the Pea Ridge Mine near Sullivan, Mo. This is an operating iron mine with an elaborate refining operation on the surface, a brief description of which is given in the April 1964 *Engineering and Mining Journal*.<sup>(21)</sup> For purposes here, a simplified and idealized geological cross section is presented in Figure 22. Also shown are the approximate transducer installation sites. The objective was to attempt transmission outside the ore body in the rhyolite porphyry, a hard, competent

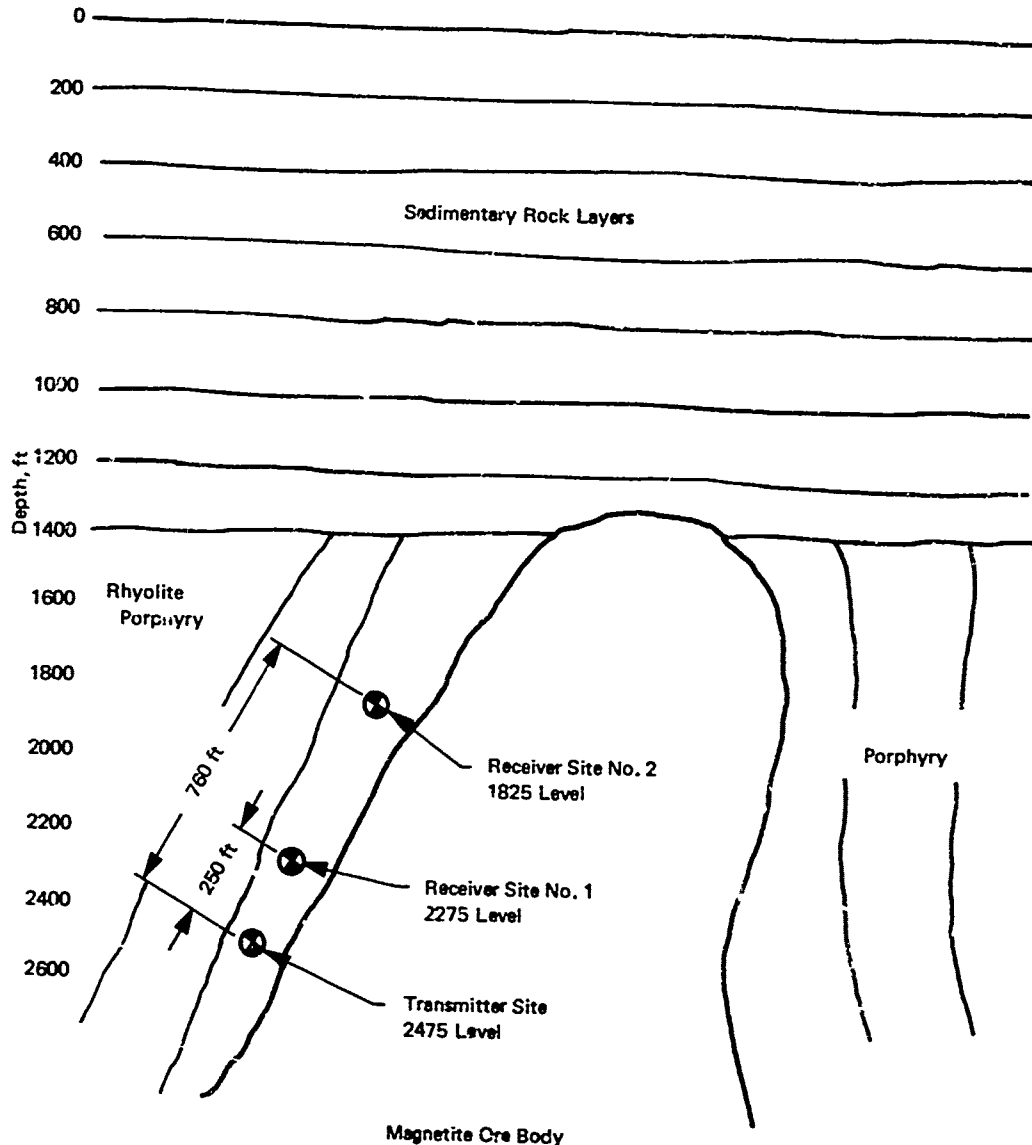


FIGURE 22. PEA RIDGE MINE--IDEALIZED GEOLOGICAL SECTION

basement rock chemically identical to granite but having finer grain structure. In consultation with the mine people, locations were selected such that no known dikes or fractures intercepted the transmission paths and for which there were no direct interconnecting paths that might support significant surface wave propagation. Other features that had to be considered included the availability of 110-VAC power at the transmitter site and of an air supply at all sites to facilitate drilling of the anchor bolt holes; relative remoteness from heavy machinery, vent fans, etc.; no interference with mine operations; and means for direct wire line interconnection between the transmitting and receiving sites. It was not possible to meet all of these requirements at each site, nor was it possible to perform the full spectrum of tests that would have been desirable. Mine management had authorized experimental work during the 2-week period covering the second and third weeks of May 1972, and it should be noted that these efforts required rather considerable support from mine personnel and consequent disruption of normal activities. The logistical and environmental difficulties associated with mounting this sort of experimental work in the far reaches of an operating mine, particularly involving the use of delicate electronic equipment, seriously limited the scope and extent of work that could be accomplished in a 2-week period. However, the intent here is not to dwell upon how these difficulties limited the work but rather to report upon what was accomplished. In sum, the transmitter unit was installed on the 2475 level, and signals were received, more or less vertically above that point, first on the 2275 level and then on the 1825 level. From directly observable results in the mine, it did not appear that an attempt to transmit over a longer path was justified. As will be shown later, that judgment was premature and incorrect. At any rate, the expiration of schedule time precluded further experimental work of significance. Summary descriptions of the experimental arrangements and results obtained follow.

## 2. TEST RESULTS

### a. Transmitter Installation: 2475 Level

One RADC transducer was installed in the back of a drift (roof of a tunnel) on the 2475 level. A photograph of this installation is presented in Figure 23. Local transmitter tests indicated that good coupling to the rock body was achieved with

$$R_p = 25,000 \text{ lb sec/in.}$$
$$C_p = 0.15 \times 10^{-6} \text{ in./lb}$$

at a resonant frequency of 308 Hz. With 1500-V rms drive, the force was 2570 lb rms, and the peak radiated power was about 30 W. The power amplifier consumed about 200 W from the 110-VAC line.

### b. Receiver Installation: 2275 Level

The other RADC transducer was installed in the rib of a drift (wall of a tunnel) on the 2275 level. From mine survey records, the vertical distance to the transmitter was 183 ft and the horizontal offset 165 ft, yielding a slant range through the porphyry of 247 ft. Local transmitter tests were not performed at this site, but later analysis of the data in the laboratory revealed that the transducer resonance was about 336 Hz at receiver signal levels. This was a distinct mismatch with the transmitter frequency of 308 Hz when the narrow band character of the devices is considered, and this points up a serious drawback in attempting to use these transducers for both transmitting and receiving. There could hardly be any doubt that the signal-to-noise ratio was diminished by perhaps 10 to 15 dB due to this detuned condition.

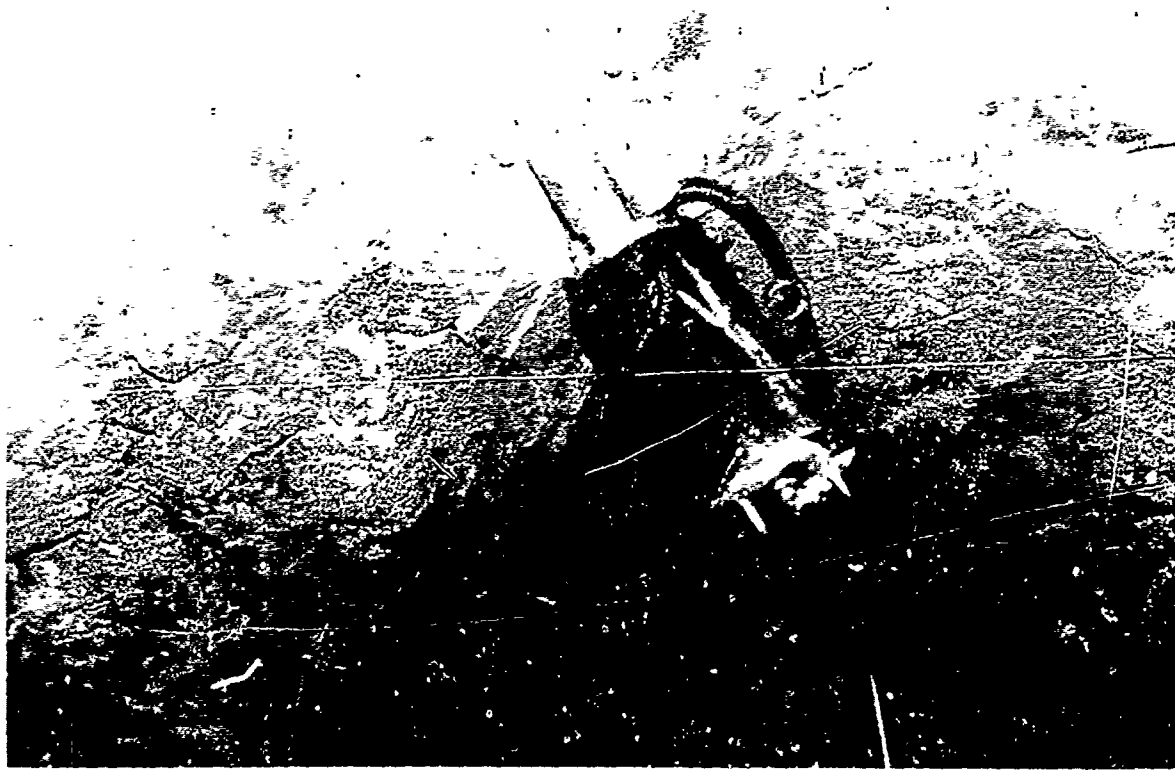


FIGURE 23. IRON MINE-TRANSMITTER INSTALLATION, 2475 LEVEL

A wire line for remote triggering was dropped down a vertical vent raise (about 6 to 8 ft in diameter) which joined the two levels at a point some 150 to 250 ft from each transducer installation. This did provide a surface wave propagation path along the drift and vent raise walls of about 600 ft with two 90-deg turns. However, from the data analysis, it is believed that little energy of significance reached the receiver by this path. At the time of the test, unfortunately, mine machinery was operating within about 200 ft of each transducer site so that there was considerable seismic and acoustic noise. Nevertheless, the transmitter was triggered a number of times and signals from the RADC transducer recorded. Triggering was very erratic, causing it to be surmised that the wire line had been damaged by mine machinery during the preceding night shift operations. Four typical recorded pulses are presented in Figure 24, the latter being obtained during a relatively quiet period. The upper trace in each case is the trigger and the lower the raw received signal. The transmit pulse was about 0.14 sec long, and this seismic input signal was assumed to be nearly identical to that obtained in the limestone quarry and given in Figure 20. Even with the extended tail on the received pulse, due to reflections, refractions, etc., a data rate of 2 to 3 pulses/sec appears quite practical.

The quiet pulse is repeated in Figure 25, stretched out timewise as an aid in determining the propagation velocity. Using the same method as employed for the quarry data and assuming the trigger actually occurred on the first transient on the trigger line, the propagation velocity was found to be over 50,000 ft/sec, an obvious absurdity since the compression wave velocity in the porphyry as calculated from physical constants of the material obtained from the mine people indicated an expected range of 19,000 to 23,000 ft/sec. Accordingly, the envelopes of the assumed input and output pulses were carefully plotted and compared with theoretical response curves, and it was found

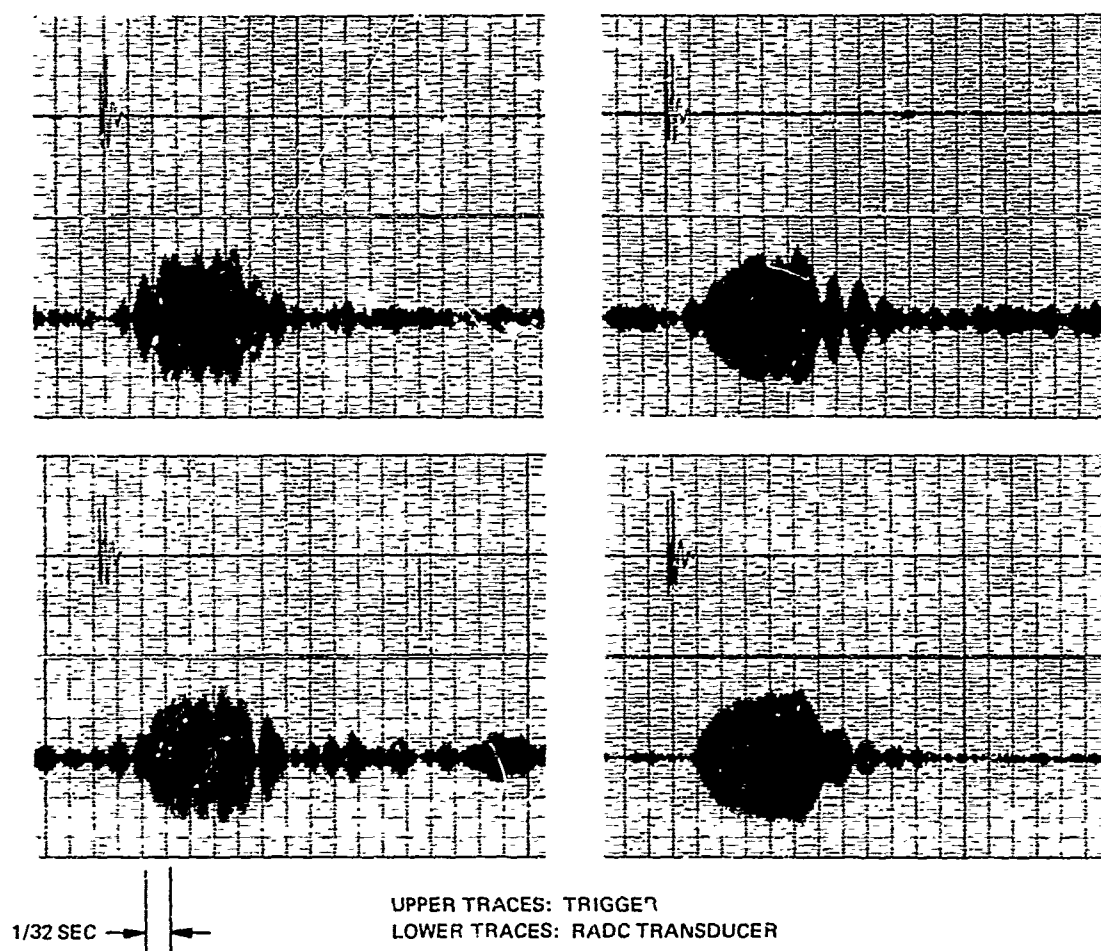


FIGURE 24. IRON MINE—TYPICAL RECEIVED SIGNALS, 2275 LEVEL

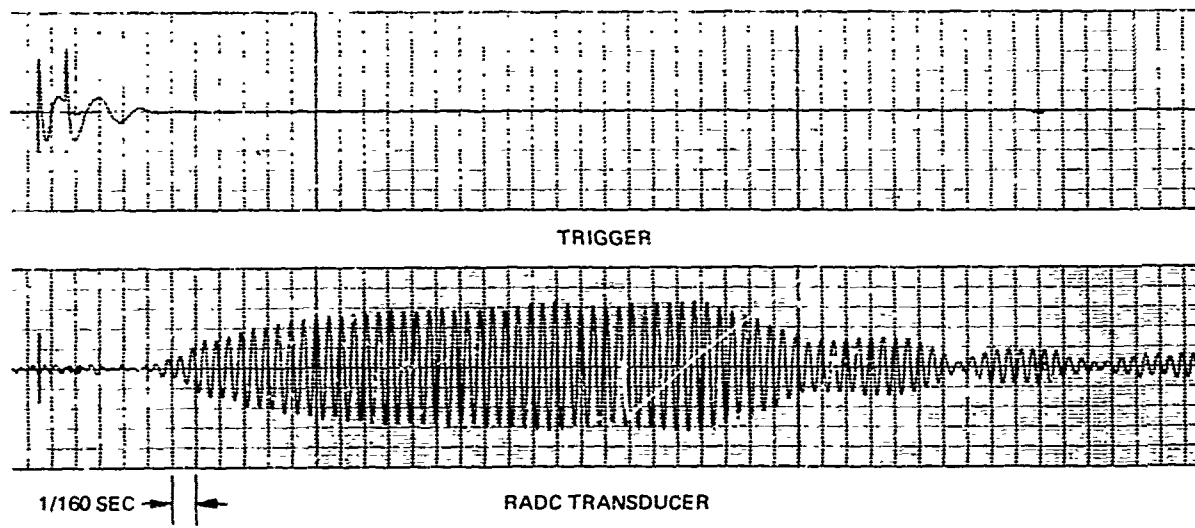


FIGURE 25. IRON MINE—TYPICAL RECEIVED SIGNALS, 2275 LEVEL

that the response more nearly corresponds to that of two first-order elements, with time constants differing by a factor of four. Thus, the time required for the input to reach 63 percent of final value corresponds to the time required for the output to reach 50 percent of final value. Using this criterion, the propagation velocity was found to be about 17,000 ft/sec. This agrees closely with the calculated values such that propagation by compressional waves is assumed. (Note that, since the propagation velocity in the magnetite ore body was less than that in the porphyry, there was no tendency to propagate a guided wave up this interface; see Owen.<sup>(1)</sup>)

With a signal-to-noise ratio approaching the order of 20 dB demonstrated (during quiet periods at least), it was decided to extend the range and attempt further communications experiments. These will be described next.

c. *Receiver Installation: 1825 Level*

A receiving site on the 1825 level was selected. This site was 642 ft vertically above and 406 ft horizontally offset from the transmitter, giving a slant range through the porphyry of 760 ft. This was a relatively quiet location. It was not feasible to interconnect the two sites with a remote trigger line; therefore, the transmitter was pulsed manually by prearranged time schedule. Figure 26 is a photograph of the receiving site on the 1825 level showing the RADC transducer affixed to the rib of the drift. Again, it was not feasible to perform local transmitter tests at this site, although later laboratory analysis of the data indicated that the installed resonance of the RADC transducer was only 260 Hz, a very "sour" installation indeed and very badly detuned with respect to the

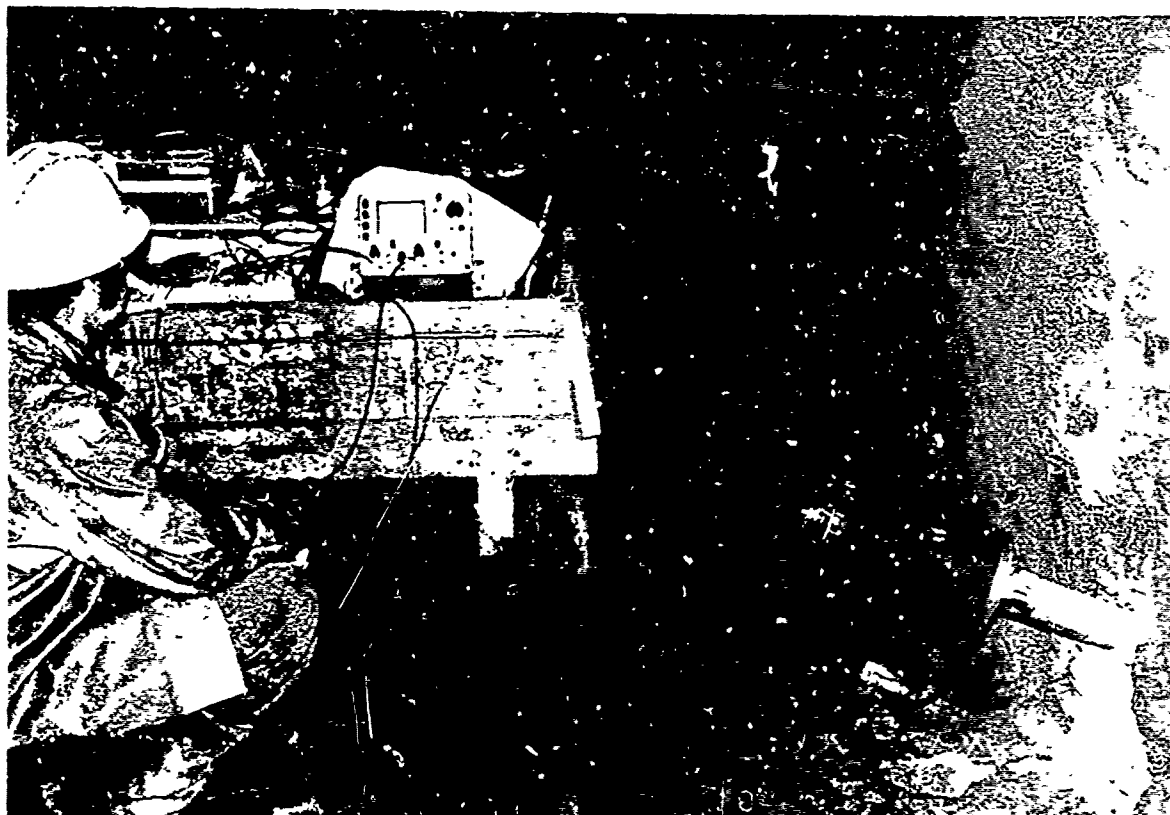


FIGURE 26. IRON MINE RECEIVER INSTALLATION, 1825 LEVEL

transmission frequency. It was remarkable that signals were received at all from this unit. The sensitive accelerometer was also used at this site, most of the time in conjunction with a filter having a 100-Hz pass band centered on 330 Hz with 24-dB/octave skirts. The accelerometer was hand held against the rock face at various points as a technique to maximize the received signal as observed on the oscilloscope.

Typical signals received by the sensitive accelerometer and the RADC transducer are shown in Figure 27. The inputs here were manually gated pulses of about 1/2-sec duration. The signal-to-noise ratios are obviously poor, particularly for the RADC transducer, although most of the raw data

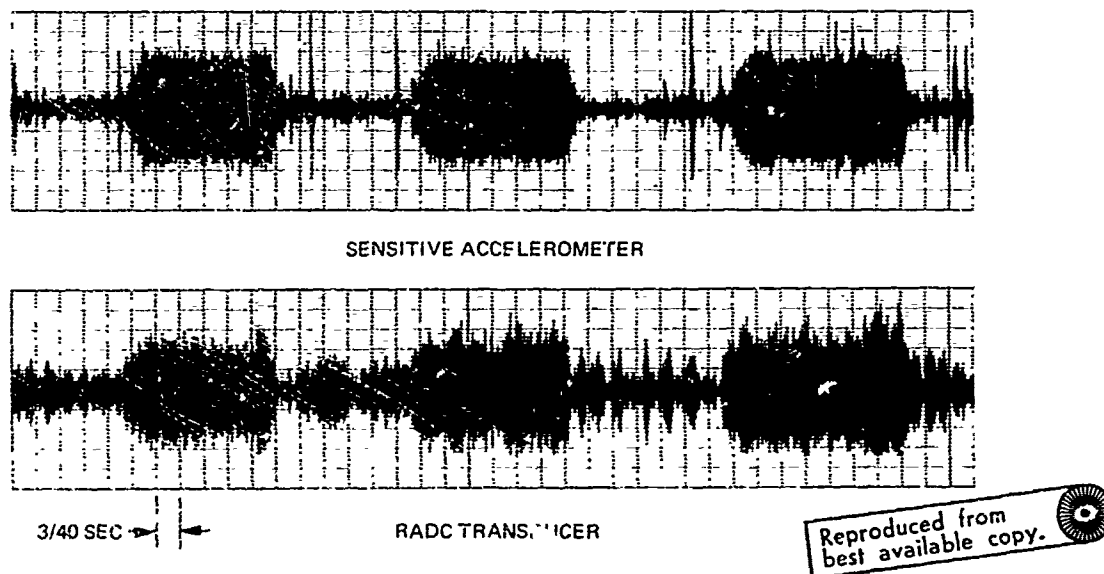


FIGURE 27. IRON MINE-TYPICAL RECEIVED SIGNALS, 1825 LEVEL

exhibited even poorer signal-to-noise ratios as will be shown later. It is of considerable interest to note that the gated pulse signal was audibly detectable by the unaided ear, though at very low level, throughout most of the test period. By use of a microphone, a short sample of this was recorded on tape. After 2 days of tests on this level, the raw data did not appear to justify a further extension of the transmission range (say by moving the receiver site to a still higher level in the mine), and so the experiments were terminated.

### 3. LABORATORY SIGNAL PROCESSING

In the laboratory, the tape-recorded signals were translated through a 32:1 time expansion and played out on a chart recorder for detailed analysis and evaluation. In addition, it was decided to attempt some signal processing to enhance the received signal-to-noise ratios. Various pass band filters were tried with moderate degrees of success, until the data were played through the narrow pass band filter of a Hewlett Packard HP 302 A wave analyzer. This filter has a pass band of 7 Hz (-3 dB) and 70 Hz (-60 dB). The results achieved were rather impressive, and typical examples are presented in Figures 28, 29, and 30. In Figure 28, the RADC transducer signal on the 2275 level is displayed along with the HP 302 A filtered signal. The improvement in signal-to-noise ratio is remarkable and approaches 40 dB for the pulse received during the quieter period. Similarly, Figure 29 presents

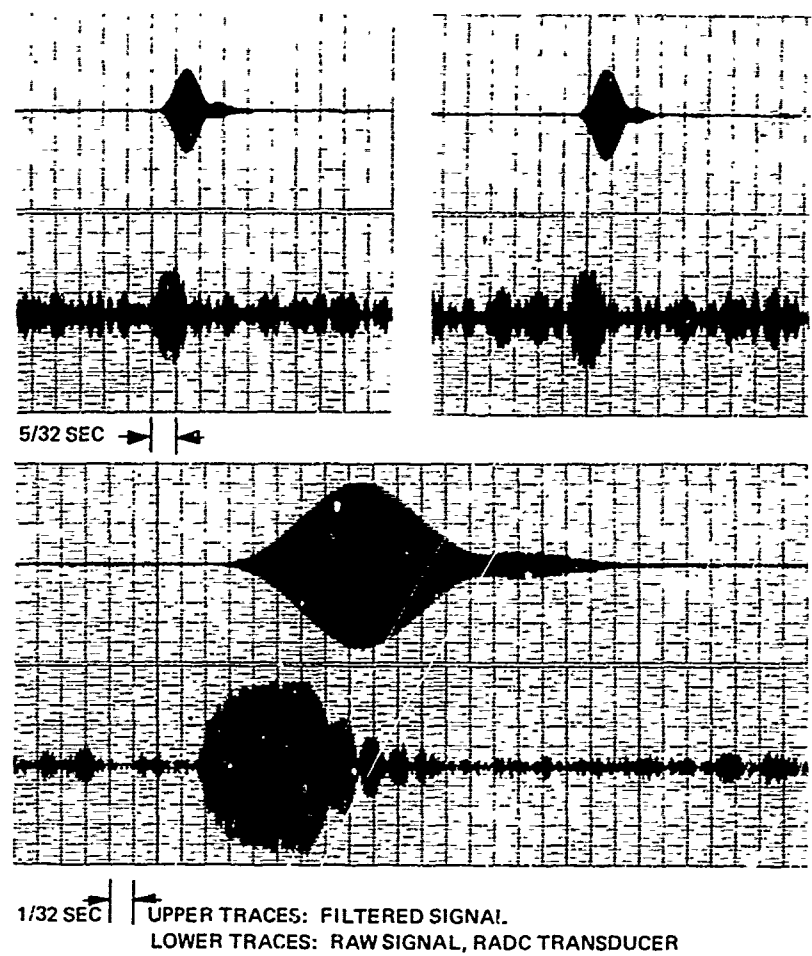


FIGURE 28. IRON MINE—NARROW BAND FILTERING, 2275 LEVEL

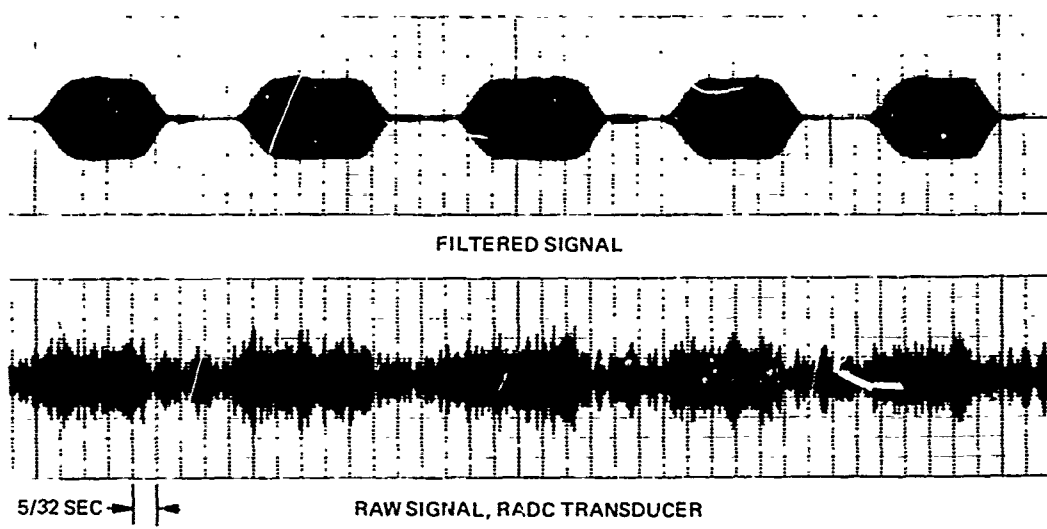


FIGURE 29. IRON MINE—NARROW BAND FILTERING, 1825 LEVEL

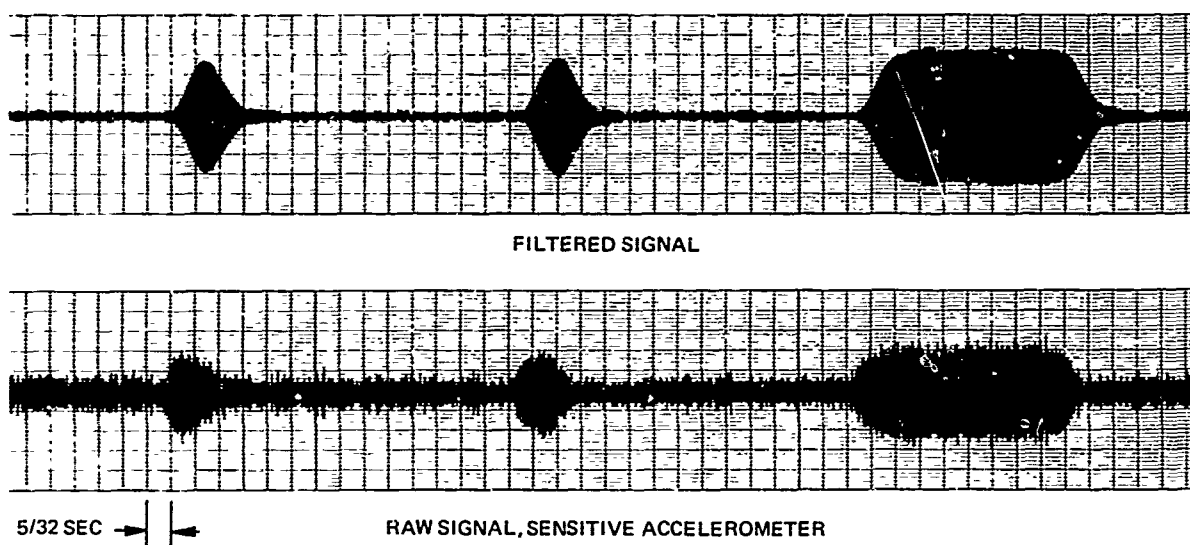


FIGURE 30. IRON MINE—NARROW BAND FILTERING, 1825 LEVEL

typical results for the filtered RADC transducer on the 1825 level. The signal-to-noise ratio in the raw signal was very poor, and, again, the improvement in the signal-to-noise ratio of the filtered signal is remarkable, perhaps exceeding 20 dB. The manually gated transmitter pulses were about 3/4 sec in duration in this example. The effect of narrow band filtering on the sensitive accelerometer signal recorded on the 1825 level is shown in Figure 30. The record shows two short pulses (about 1/4 sec each) and one long pulse (about 1 sec), such as might be used in a coded message. It is seen that the narrow band filter does give a lagged response, but the rise time of the otherwise Q-limited pulse is not greatly increased. A data rate of two pulses/sec appears to be quite practical even with a narrow band filter of the type employed here.

#### 4. SIGNAL ATTENUATION WITH RANGE

Relative received signal levels on the 2275 and 1825 levels were compared for purposes of estimating signal attenuation loss in the seismic medium. The loss was estimated to be about 15 dB, although the accuracy of the data is open to serious doubt since the RADC receiving transducer was detuned at both receiving sites to differing degrees. Unfortunately, because of equipment difficulties at the time, the sensitive accelerometer signal was not recorded on the 2275 level.

## SECTION VI

### CONCLUSIONS AND RECOMMENDATIONS

Results of communications experiments in an operating iron mine have shown that the RADC piezoelectric transducer performed quite well as a source or transmitter for radiating communications-type gated pulse signals into hard, competent rock media. For a peak radiated power of about 30 W, signals were received at a distance of 760 ft through hard rock, which, after being processed through a narrow band filter tuned to the transmitter unit frequency, exhibited a signal-to-noise ratio of the order of 20 dB and a data rate capability of about two pulses/sec. These results taken together with the results of the theoretical analysis, laboratory tests, and other field tests lead to the following conclusions:

- (1) A piezoelectric transducer, loaded by a high Q spring-mass resonator on the air side, by proper design can be efficiently coupled (or impedance matched) to hard, competent rock media for the purpose of radiating seismic signals into the media.
- (2) The power conversion efficiency of such a source transducer can be made about 70 to 80 percent, while overall power conversion efficiency employing a class B, solid-state driver can be made to approach 50 percent.
- (3) Because of the narrow operating bandwidth of such a high Q transducer, pulse width or pulse code modulation techniques are indicated, and data rates will be limited to a few pulses per second.
- (4) Transducer resonant frequency of about 300 Hz is probably a good compromise between power radiating capability and attenuation loss in hard rock seismic media. However, definitive data to support this statement were not generated in this effort.
- (5) Such a transducer is not suitable for use as a receiver because of the variations in installed resonant frequency at each site. A sensitive receiver such as an accelerometer or geophone, exhibiting say a 50-Hz bandwidth, would be a better selection.
- (6) To maximize the signal-to-noise ratio, particularly in noisy environments, the received signals should be filtered by a very narrow band filter tuned to the transmitter unit resonant frequency.
- (7) Seismic propagation through highly fractured media will result in large attenuation losses and should be avoided if possible.
- (8) Attachment of the transducer to the rock medium interface should be done very carefully to insure good coupling. The coupling should be verified by performing power radiation tests and the transducer moved and reinstalled if indicated.
- (9) In massive hard rock, effective seismic communication ranges of 1000 ft or greater should be practical with total peak power consumption of 100 W.

- (10) For shorter seismic transmission paths through rock, higher frequencies could be employed with correspondingly increased data rate capabilities. Depending upon the frequency selected and the signal attenuation in the rock, this might require more or less power radiating capability than the current RADC transducer. For sufficiently short, low-loss paths, a nonresonant, broadband piezoelectric transducer might become feasible.
- (11) Adaptation of existing technology in piezoelectric transducers and in electronic techniques and equipment to this application is straightforward.

The above conclusions are meant to demonstrate the feasibility of employing this type of piezoelectric transducer to seismic communications, at least within the limits specified. Since the relative success of such an application is highly dependent upon the seismic propagation characteristics of a given transmission path of interest, it is recommended that preliminary communications tests be performed at any such site before finalizing of design and equipment parameters.

Further, such tests could be greatly facilitated and the design of a final transducer further advanced by developing an improved version of the current RADC transducer. Specifically, the objectives for such a development would be as follows:

- (1) Increased radiating power capacity;
- (2) Elimination of nonlinearity problem;
- (3) Reduction in size and weight;
- (4) Design of a ruggedized electronics drive and receiving system.

## APPENDIX

### DERIVATION OF PIEZOELECTRIC CRYSTAL EQUIVALENT CIRCUIT

Consider a piezoelectric crystal of thickness,  $\ell$ , and cross sectional area,  $a$ , driven in the thickness mode, and neglect radial and other modes. As given by Gooberman<sup>(18)</sup> or Mason<sup>(19)</sup>, the applicable piezoelectric equations are

$$T_x = C_x^D \frac{\partial \xi_x}{\partial x} - h D_x \quad (22)$$

$$E_x = \frac{1}{\epsilon_x^s} D_x - h \frac{\partial \xi_x}{\partial x} \quad (23)$$

where

- $T_x$  — tension in crystal along the  $x$  direction, N/m<sup>2</sup>
- $C_x^D$  — elastic constant along the  $x$  direction at constant charge density, N/m<sup>2</sup>
- $\xi_x$  — crystal displacement along  $x$  direction, m
- $h$  — piezoelectric constant, V/m or N/C
- $D_x$  — charge density in  $x$  direction, C/m<sup>2</sup>
- $E_x$  — electric field in  $x$  direction, V/m
- $\epsilon_x^s$  — absolute permittivity in  $x$  direction at constant material strain, F/m

MKS units are shown since this system of units is somewhat more convenient to work with.

Eqs. (22) and (23) express the relationships among the electrical and mechanical conditions at a given point within the crystal. If the propagational wavelength is very long compared to the crystal thickness,  $\ell$  along the  $x$  direction (such as is the case here; i.e., the wavelength in PZT-4 material at 350 Hz is about 38 ft), then the equations become, upon dropping the subscript,  $x$ ,

$$T = C^D \frac{\Delta \ell}{\ell} - h D$$

$$E = \frac{1}{\epsilon^s} D - h \frac{\Delta \ell}{\ell}$$

where  $\Delta \ell$  is the total expansion in crystal thickness. Multiplying the first by the area,  $a$ , gives

$$F = k \Delta \ell - h Q \quad (24)$$

where

$$k = \frac{C^D a}{\ell}, \text{ the short circuit spring rate of the crystal}$$

$$Q = Da, \text{ free charge on crystal}$$

and  $F$  is the tension force across crystal. Multiplying the equation for  $E$  by the thickness,  $\lambda$  gives

$$V = \frac{Q}{C_o} - h\Delta\ell \quad (25)$$

where  $V$  is the voltage across crystal and

$$C_o = \frac{\epsilon^s a}{\lambda}, \text{ clamped capacitance of crystal}$$

Combining Eqs. (24) and (25) to eliminate  $Q$  and using a compressive force

$$F_c = -F$$

yields

$$F_c = hC_o V - \Delta\ell(k - h^2 C_o) \quad (26)$$

For various reasons, it is convenient and customary to work with the concept of impedance, both electrically and mechanically, where electrical impedance is the ratio of voltage to current and mechanical impedance is the ratio of force to velocity. This implies the following analogical correspondence:

$$\begin{aligned} \text{voltage} &\rightarrow \text{force} \\ \text{current} &\rightarrow \text{velocity} \\ \text{charge} &\rightarrow \text{displacement} \end{aligned}$$

and, derivatively,

$$\begin{aligned} \text{capacitance} &\rightarrow \text{inverse spring rate} \\ \text{inductance} &\rightarrow \text{mass} \\ \text{resistance} &\rightarrow \text{viscous damping} \end{aligned}$$

Thus, if sinusoidal time variation at radian frequency,  $\omega$ , is assumed and velocity is defined

$$v = j\omega\Delta\ell$$

and current is

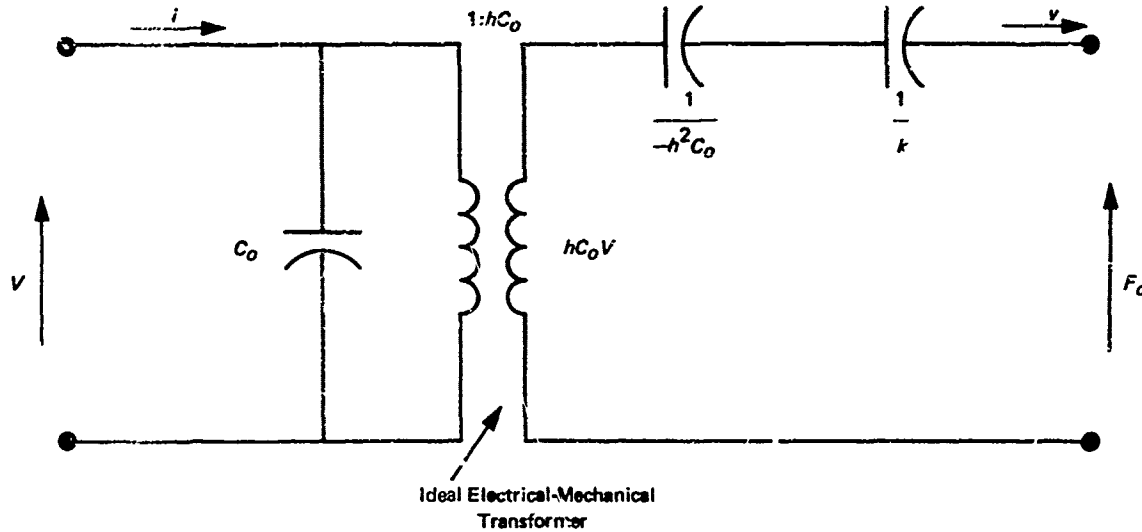
$$i = j\omega Q$$

then Eqs. (25) and (26) become, upon some rearranging,

$$i = j\omega C_o V + hC_o v \quad (27)$$

$$F_c = hC_o V - \frac{v}{j\omega} (k - h^2 C_o) \quad (28)$$

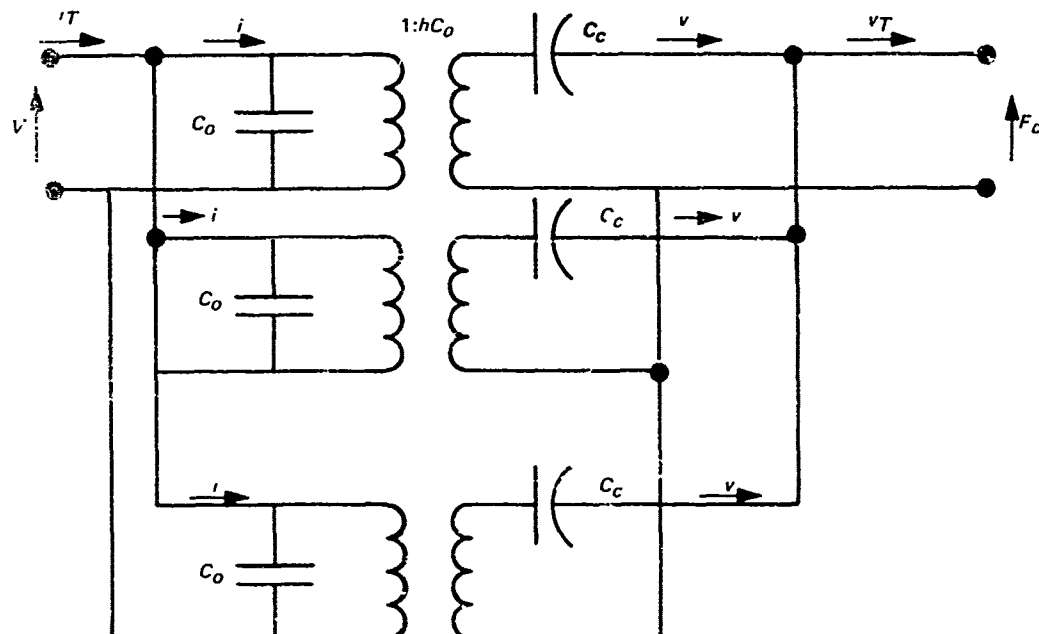
These equations suggest the following equivalent circuit:



All quantities to the left of the transformer are electrical, while all quantities to the right are mechanical. The mechanical "capacitors" are proportional to inverse spring rates, one of which represents the elastic spring rate of the crystal when electrically shorted and the other a negative spring rate associated with the change in free charge resulting with constant voltage excitation. These two capacitors shall be combined into a single capacitor in what follows.

For  $n$  crystals, stacked mechanically in a series but connected electrically in parallel, the following equivalent circuit is suggested, where

$$C_c = \frac{1}{k - h^2 C_0}$$



It is evident that the total current is

$$i_T = ni$$

the output velocity is

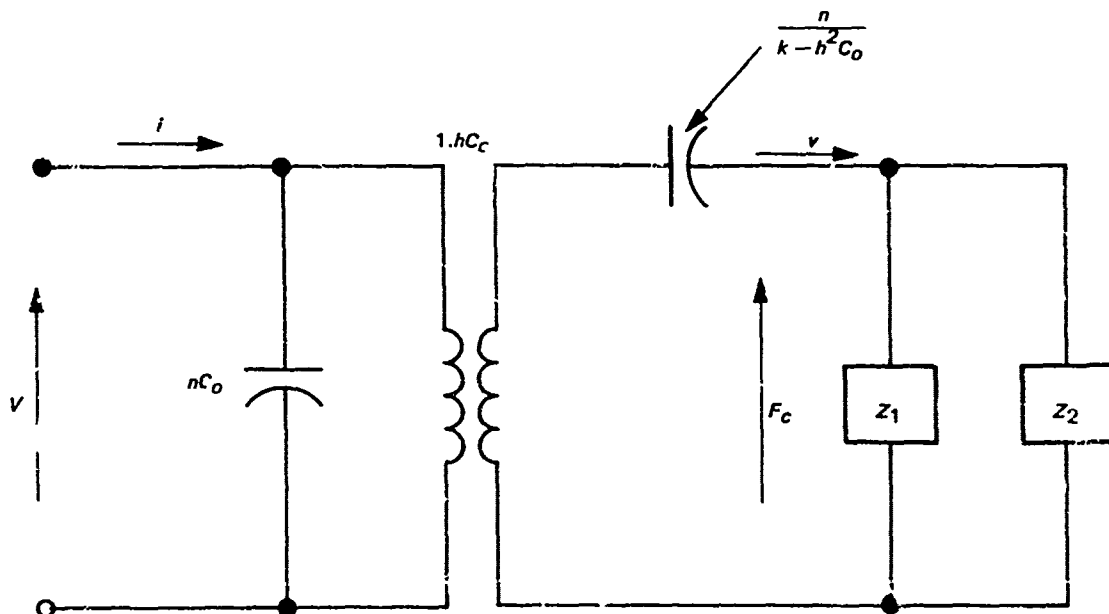
$$v_T = nv$$

and the output force,  $F_c$ , across the entire stack is the same as the force across a single crystal. Consequently, Eqs. (27) and (28) become, for a stack of  $n$  crystals,

$$i_T = j\omega n C_o V + h C_o v_T \quad (29)$$

$$F_c = h C_o V - \frac{v}{j\omega n} (k - h^2 C_o) \quad (30)$$

and the final equivalent circuit is given as follows where we have now added a mechanical load to each end of the crystal stack represented as mechanical impedances  $Z_1$  and  $Z_2$  and have dropped the subscripts on  $v$  and  $i$ :



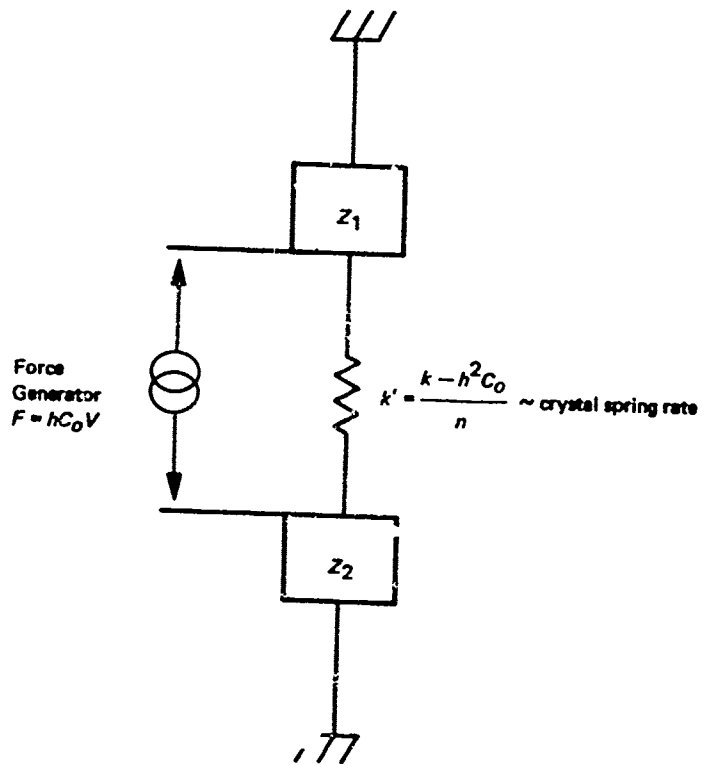
Alternatively, the mechanical portion of the circuit might be depicted by using mechanical elements as shown on the following page.

From manufacturers' published data, numerical constants for the crystal stack are as follows:

$$\begin{aligned} n &= 6 \\ a &= 2.85 \text{ in.}^2 = 0.00184 \text{ m}^2 \\ l &= 0.2 \text{ in.} = 0.00508 \text{ m} \end{aligned}$$

$$\begin{aligned}
 \epsilon^s &= 5680 \times 10^{-12} \text{ F/m} \\
 C_o &= 0.00204 \mu\text{F} \\
 nC_o &= 0.0122 \mu\text{F} \\
 h &= 3.15 \times 10^9 \text{ V/m (N/C)} \\
 C^D &= 12.66 \times 10^{10} \text{ V/m}^2 \\
 k &= 4.58 \times 10^{10} \text{ N/m} \\
 hC_o &= 6.42 \text{ N/V (A sec/m)} \\
 h^2C_o &= 2.03 \times 10^{10} \text{ N/m}
 \end{aligned}$$

$$C_c = \frac{n}{k - h^2 C_o} = 2.35 \times 10^{-10} \text{ m/N}$$



## REFERENCES

1. Owen, T.E., *A Feasibility Study of Communication by Means of Elastic Wave Transmission Through the Earth*, Ph.D. Thesis, The University of Texas, 1964.
2. Evison, F.F., "A New Approach to the Study of Elastic Propagation in Rocks," *Mon. Not. Roy. Astron. Soc., Geophys. Suppl.*, Vol. 6, 1951.
3. Evison, F.F., "An Electromechanical Source of Elastic Waves in the Ground," *Proc. Phys. Soc. (London)*, Sect. B., Vol. 64, April 1951.
4. Evison, F.F., "An Improved Electromechanical Seismic Source Tested in Shattered Rock," *New Zealand Jour. Sci. and Tech.*, Vol. 35, No. 1, 1954.
5. Evison, F.F., "A Coal Seam as a Guide for Seismic Energy," *Nature*, Vol. 176, 1955.
6. Evison, F.F., "Seismic Waves from a Transducer at the Surface of Stratified Ground," *Geophys.*, Vol. 21, No. 4, October 1956.
7. Evison, F.F., "Pulsed Vibrator as Seismic Source," *Geophysical Prosp.*, Vol. 5, No. 4, December 1957.
8. Pursey, H., "Motional Impedance of Simple Sources in an Isotropic Solid," *British J. App. Phys.*, Vol. 4, 1953.
9. Miller, G.F., and Pursey, H., "The Field and Radiation Impedance of Mechanical Radiation on the Free Surface of a Semi-Infinite Isotropic Solid," *Proc. Roy. Soc. (A)*, Vol. 223, 1954.
10. Miller, G.F., and Pursey, H., "On the Partition of Energy between Elastic Waves in a Semi-Infinite Solid," *Proc. Roy. Soc. (A)*, Vol. 233, 1955.
11. Pursey, H., "Power Radiated by Electromechanical Wave Source," *Phys. Soc. Proc. (B)*, Vol. 69, pt. 2, No. 434-B, February 1956.
12. Ikrath, K., and Schneider, W., "Communication Via Seismic Waves," USAELRDL Tech. Report 2346, May 1963.
13. Ikrath, K., and Schneider, W., "The Realization of Active Seismic Systems and Their Practical Applications," USAELRDL Tech. Report 2446, April 1964.
14. Ikrath, K., et al, "Active Seismic Systems for Communications and Surveillance," ECOM Tech. Report 2695 (AD-632082), April 1966.
15. Ikrath, K., Schneider, W., and Johnson, R., "Transmitier Arrays in Active Seismic Systems for Communications and Surveillance," ECOM Tech. Report 2730, June 1966.
16. Zeitz, I., and Pakiser, L.D., "Note on Application of Sonar to Shallow Reflection," *Geophys.*, Vol. 22, No. 2, April 1957.

17. McMaster, R.C., et al, "Development of Sonic and Ultrasonic Power Devices for Application in Highway Engineering," Final Report, Project EES220, Ohio State University, August 1970.
18. Gooberman, G.L., **Ultrasonics: Theory and Application**, Hart Publishing Co., New York, 1968.
19. Mason, W.P., **Piezoelectric Crystals and Their Application to Ultrasonics**, D. Van Nostrand Co., New York, 1950.
20. Lypacewicz, G., and Filipczynski, L., "Measurements of the Clamped Capacitance  $C_o$  and the Electromechanical Coupling Coefficient  $k_t$  of Ceramic Transducers under Mechanical Load," *Acustica*, Vol. 25, No. 1, July 1971.
21. Anonymous, "Meramec Iron Ore Project Starts Production at Pea Ridge," *Engineering and Mining Journal*, Vol. 165, No. 4, April 1964.